ECOLE POLYTECHNIQUE FEDERALE DE LAUSANNE SCHOOL OF LIFE
SCIENCES



MASTER PROJECT IN LIFE SCIENCES ENGINEERING

# Comparing neural responses between action execution and action perception

Carried out in the Kreiman Laboratory,
Harvard Medical School, Boston,
Under the supervision of Gabriel Kreiman, PhD.

DONE BY

## YAEL PORTE

UNDER THE DIRECTION OF:
PROF. GREGOIRE COURTINE
IN THE LABORATORY G-LAB UPCOURTINE

EPFL

EXTERNAL EXPERT: PROF. GABRIEL KREIMAN

LAUSANNE, 4 MARCH 2022

# Contents

# Acknowledgements

First thing first, I would like to express my gratitude towards my supervisor, Gabriel Kreiman [1], who has given me the opportunity to conduct my Master's thesis in his laboratory and mentored me throughout the completion of this project. I especially appreciated the warm and welcoming atmosphere that reigns within the lab thanks to him. A special thank you goes to Marcelo Armendariz, Pranav Misra, David Mazumder and Yuchen Xiao for always taking the time to help me, for their patience and kindness. I wish to thank Marcelo for his infinite patience and true kindness that helped me carry out this project. I also truly appreciated Pranav for providing me great guidance and advice for my first experiment with patients. I also would like to thank Antonino Casile [2] for overviewing my project every week, for being always available, despite the jetlag and geographic separation. I felt really lucky to work alongside with Dr. kreiman and Dr. Casile and benefit from Gabriel Kreiman's extensive experience in studying cognitive processes in epilepsy patients and Antonino Casile's vast experience in investigating action perception both at neuronal and behavioral levels. Furthermore, they both have a history of supervising EPFL student's master's thesis. I also wish to show appreciation towards Edward Soucy for his help regarding my equipment, his immense kindness and availability. Last but not least I would also like to thank my EPFL supervisor, Gregoire Courtine [3], to kindly have accepted to oversee this project.

---

[1]Department of Ophthalmology, Boston Children's Hospital, Harvard Medical School, Boston, USA
[2]Center for Translational Neurophysiology, Instituto Italiano di Tecnologia, Ferrara, Italy
[3]G-lab upcourtine, EPFL, Lausanne, Switzerland

# List of Figures

# List of Tables

## Abstract

*The goal of this master's thesis is to give insight into the neural mechanisms that allow us to perceive and understand actions of others, which is critical to engage in social interactions. Many studies suggest that mirror neurons are at stake when it comes to action perception. However, this is still up to debate and this matter hasn't been studied rigorously in humans using intracranial techniques.*

*To further study the question of mirror neurons at intracranial level in humans, power modulations of local field potentials recorded from SEEG responses in patients with intractable epilepsy were analyzed during action execution and compared to the visual responses during action perception of the same action. We observed three frequency ranges that encode important information both for motor and visual responses. High frequencies (between 45 and 70 Hz-gamma band) and low to mid frequencies (0.1 to 8Hz- delta and alpha bands) induce a power peack related to movement. A power drop between 15 Hz to 25 Hz (beta band) is associated with movement preparation and execution. These modulations in neural responses were find similar between action execution and action perception in the low to mid frequency band, but significantly different in the beta and gamma bands. The grip types are encoded in gamma bands. Even though this study was only conducted on one patient and the significance can be questioned, this gives a first understanding of the comparison between action execution and observation of three different types of grips and opens the door for exciting findings.*

## 1   Introduction

This Master's Thesis is the continuity of Alice Motschi master's project that she conducted in the Kreiman Lab in 2019. One the most remarkable and notorious ability of human beings is their great action perception skills that allow them to engage in very complex social interactions. Everyday, we perform many joint actions (which is defined by Sebanz et al. as any form of social interaction whereby two or more individuals coordinate their actions in space and time to bring about a change in the environment [1]). This requires to not only be able to understand and monitor others' actions at a certain point in time, but also to interpret them, understand them in a context and predict the outcomes of their actions and what they are going to do next in order to adopt the best complementary behavior. This capacity calls for a high level of visual analysis and understanding of others actions. This is an incredibly complex task, from a computational point of view at least, that our brain seems to be doing effortlessly. Furthermore, unlike other species, we, as humans, are able to learn by imitation [2].

Therefore, we can wonder what are the neural and cognitive processes that enable our brains to perceive so smoothly the movements of others, link action understanding to a particular context, and with such a high level of details. Why do we react so instinctively to other people's actions. How do we understand almost immediately their thoughts, feelings and intentions? What mechanisms allow this imitation learning?

In the last decades, a multitude of studies have demonstrated the existence of a mirror neuron system in the human brain, which fire both when executing actions and when observing the same actions done by other individuals. This dual property earned them the designation of "revolution in understanding social behaviour" by C. Heyes [3]. This is thought to explain how we perceive others actions. Indeed, when we see someone else doing an action, the involved neurons gets activated, and as we know the outcome of those neurons when activated, we understand what the other person is doing [REF]. This could also explain why humans are able to show empathy for others and learn through mimicry: if

1

watching an action and performing that same action can activate the dentical parts of the brain, then it's logical that watching an action can bring out similar feelings in people then when executing this action. Nevertheless, this topic is still up for discussion and we still haven't been able to prove that humans have individual mirror neurons.

Finally, the questions that will be explored in this project are: Which regions of the brain encode for action execution and action perception? Are they the same? Which modulations in the neuronal responses are characteristic for movement execution and preparation ? Are these same mechanisms present not only in motor responses, but also in visual responses ? What is the dynamic of these mechanisms, meaning when exactly do these neural modulations occur? Is the dynamic the same during action execution and action perception? Can we detect in humans the presence of neurons that fire during action execution and action perception at the level of intracranial field potential ?
Is the intermediate goal of the action (meaning the grip type) encoded in visual responses? To answer these questions, I will first design and run experiments with patients at the Boston Children's to collect physiological data. In a second part, I will perform a data analysis to explore the motor responses recorded and look out for characteristics specific for frequency bands during movement execution and preparation. These characteristics will then be compared to those of visual responses at different levels of depth in different areas of the brain.

## 2 Theoretical background

### 2.1 Mirror Neurons

Mirror neurons were first discovered in the early 1990s by neuroscientist Giacomo Rizzolatti, MD, and his colleagues at the University of Parma. Their researchs allowed to shed light on a consistent percentage of neurons in the premotor cortex (area F5) of macaque monkeys that transmit electrical impulses not only when monkeys carry out purposeful object-oriented motor actions, but also during observation of the equivalent action being done by another monkey or a human. [4] [5]. This discovery can almost be considered fortuitous. Rizzolatti et al. first found that some neurons in the F5 area of monkeys fired when the monkeys did simple reaching actions. To learn more about these neurons responses to different types of objects and actions, they used electrodes to record activity from individual F5 neurons while handing the monkeys different objects to manipulate. This is how they discovered that when they picked up an object to give it to the monkey, some of the monkey's motor neurons would become active and as a matter of fact, these were the same neurons that would also fire when the monkey itself grasped the same object. The team observed that individual neurons responses were action-specific. For example, a neuron that fired when the monkey handled a peanut would fire only when the experimenter handled a peanut as well. Whereas a neuron that fired when the monkey eats the peanut would only fire when the experimenter eats the peanut too [4] [6].

Neurons with the same mirroring properties have been later discovered also in the inferior parietal lobule of the monkey [7] [8] [5]. This proves that the parietal cortex, that was up until now only considered an association cortex, is also involved in the execution and interpretation of motor actions.

Beyond this congruent visuomotor responses property, these findings revealed other interesting characteristics of mirror neurons. First, mirror neurons seem to be activated only by biological motions. Indeed, they did not respond when grasping was achieved using artificial tools such as pliers for example. Second, mirrors neurons could also fire by hearing the sound of a particular action so the activity of the mirror neurons are triggered by the meaning and not by the visual features of the observed action. Finally, activation of mirror neurons requires the achievement of the goal of the action. For instance, the observation of fake grasping in the absence of an object, or of the object but without any grasping action,is not enough to induce

mirror neurons discharge [9]. The last property gives the assumption that mirror neurons participate, at least to some level, in understanding the intention underlying action.

In this study from 2005 [8], Fogassi et al. suggested that mirror neurons in the inferior parietal cortex may be responsible for encoding the context under which actions occur, helping us understanding the intentions behind other's action.

Gentilucci and Rizzolatti later showed that the F5 area codes for detailed movements of the hand such as 'precision grip', 'finger prehension' or 'power grip' [5] [10], whereas the neurons in IPL encode more generic actions such as 'grasp', 'reach' or 'place'.

Given the homology between F5 area in monkeys and human Brocca's region, Rizzolati et al. suggested that a similar system exists in humans [11]. The next step was then naturally to try and prove it.
When conducting experiments with humans, non-invasive techniques such as EEG (electroencephalography), MEG (magnetoencephalography), or magnetic-resonance imaging (fMRI) are often used to record brain activity as they are much simpler to use due to reduces ethical restrictions and more subjects available. However, they lack in precision and make it difficult to distinguish simultaneously occurring processes. Invasive techniques like ECoG (electrocorticography), SEEG (stereo EEG), or stimulated the nervous system using TMS (transcranial magnetic stimulation) are less commonly used but allow to overcome these matters. Thanks to the previously cited techniques, researchers were able to provide evidence of a mirror neuron system in the human brain [2] [12]. The first human mirror neuron study were conducted by Rizzolatti et al. Motor-evoked potentials were recorded from participants' hand muscles while the participants were asked to grasp object and watch the experimenter grasp objects. They found that potentials recorded in both cases matched [13]. In their study, Frith and Frith showed that medial prefrontal cortex and posterior superior temporal sulcus were implicated as components of this system [14] while J. Grezes et al. found neu-

rons that were activated in the dorsal premotor cortex, the intraparietal cortex, the parietal operculum, and the superior temporal sulcus when subjects observed gestures [15]. M. Iacoboni et al., used fMRI to image the brain activity of participants while they watched experimenters make movements with their finger and while they did the same finger movements themselves. The team found two areas that became active during movement execution and observation in the left inferior frontal cortex (opercular region) and the rostral-most region of the right superior parietal lobule [16].

However, even if evidence of a mirror neurons system have been found in humans, there is still a scale difference between the imaging studies in humans and the electrophysiological studies in monkeys. If we can record signals in monkeys at a single neuron level, in human we can only show that there is activation within a small area that contains millions of neurons, meaning that it is impossible to know for sure if it's really the same neuron that is firing in both cases or if it's simply neigbhors neurons in this small area [6]. It is yet to prove the existence of individual mirror neurons in humans.

## 2.2 Specific frequency bands-dependant modulation of neural activity

The electric potential in the extracellular space in brain tissue can be recorded through SEEG electrodes. This potential is referred to as Intracranial Field Potential (IFP). IFPs are recorded in depth (from within the cortical tissue or other deep structures). This is where it differs from the EEG, which is recorded at the surface of the scalp IFP constitutes a good measure for brain activity. Indeed, IFP signals are believed to reflect neural action potential activity, and their frequency modulations are associated to spiking events [17]. IFP analysis is done by computing power spectra densities of these signals in different frequency bands where most of the information is usually contained in lower frequency bands [18]. Historically, frequency bands are described as follows: $\delta$—delta band (less than 4

Hz), $\theta$—theta (4–7 Hz), $\alpha$—alpha (8–15 Hz) (occasionally $\mu$—mu (8–12 Hz)), $\beta$—beta (16–31 Hz), $\gamma$—gamma (more than 31 Hz) (dissociated between $\gamma$-gamma (30–80 Hz) and high $\gamma$-gamma (80–150Hz)) [19] [20] [21]. For cortical IFPs, the frequencies ranges can span from less than one Hz to more than one hundred Hz. Therefore, IFPS contain a broad spectrum of fluctuations of neural activity and their different band-limited components allow to capture a multitude of neural processes Recording and analysing IFPs give insights into the circuit mechanism generating neural representation of information. Finally, IFPs provide stable signal for a long period of time [?].

Depending on the frequency band, different neuronal events can be observed and delta, theta and gamma bands have been shown to be the most informative ranges [22]. Gamma activity is linked to specific motor skills and movements. It was demonstrated that the power in the gamma band increases in the primary motor cortex during motor tasks (like reaching for example) and during cognitive processes [23] [24]. Motor gamma oscillations have also been observed for simple and small movements, like finger movements (precision grip), tongue protrusions, eye-winking or fist-clenching [24] [25] [26] [27] [28], but also for more elaborate movement such as walking or cycling [29] [30].

We can also see modification in the amplitude of other frequency bands during motion or cognitive processes. Indeed, the amplitude of alpha and beta bands has been shown to decrease during reaching tasks [24], [31], [32] [33]. whereas theta oscillations with high amplitude have been observed in the human brain during perceptual and cognitive processes. The interesting thing is that we can see these changes not only during the execution of these motions, but also when their are imagined or perceived [34]. We could also see beta desynchronization during movement preparation in the supplementary motor area [31]. Beta activity is characterized by increasing before the onset of movements, declining during the movement, followed by a re-synchronization after movement [35] [36]. The explanation behind these observations can be that the phase of lower frequencies, like theta, alpha and beta bands, would modulate fast gamma oscillation powers allowing to synchronize fast processes like movements with slower processes like perception and cognition [37] [31].

# 3 Material and Methods

## 3.1 Data collection

### 3.1.1 Subjects

The experiments were carried out on 3 patients (2 males and 1 female; age $11 \pm 3$ years old) suffering from refractory epilepsy (drug-resistant). The patients were hospitalized for the purpose of identifying their epileptogenic zones (which was defined in 1993 by Luders et al. as "the area of brain that is necessary and sufficient for initiating seizures and whose removal or disconnection is necessary for abolition of seizures" [38]. The goal is to localize seizure foci in order to later perform surgical resection to eliminate the seizures.

Different recording methods allow to do this. The most common non-invasive method is scalp electroencephalography (EEG). This technique is widely used in humans because it is functionally fast, cheap, easy and safe to implement. However, EEG recordings offer poor spatial resolution and won't allow pin-pointing the exact source of activity. EEG electrodes are simply attached onto the scalp and therefore the signal is blocked by the skull, the skin, and other high resistance tissues [39]. For a higher resolution, two more invasive approaches exist: Wilder and Penfield's use of subdural grid and strip electrodes for electrocorticography (ECoG) developed in 1956 versus Talaraich and Bancaud's approach of using purely depth electrodes in stereo EEG (SEEG) pioneered in Paris in 1965 [38] [40]. With both these techniques, we can detect two of the most important features of intracranial recordings, broadband gamma activity and low-frequency oscillatory activity [41]. The choice between these two methods depends on clinical need. In our case, the three patients were implanted with intracortical electrodes SEEG (PMT Corporation, Chanhassen, MN, USA, see Figure 18 in Annex). In SEEG, instead of placing electrodes on the lateral surface of the cortex, SEEG inserts depth electrodes into the human brain. This technique allows to sample the temporal evolution of neural activity at many

locations [41]. The electrodes are implanted using robotic assistance, which reduce the surgical trauma (burr holes instead of a full craniotomy [41]) [42]. Their location is determined based on estimations where surgeons evaluate the seizures might be starting, following non-invasive tests, and is adapted to each patient individually [43]. The locations of the electrodes are entirely based the meet the requirements of the clinical evaluation but in our cases they were localized over prefrontal, motor, temporal or parietal areas. The electrodes penetrate the brain and provide a sparse sampling of a unique set of brain regions. They can record from deeper brain structures such as hippocampus, amygdala and insula that cannot be captured by superficial measurement modalities such as electrocorticography (ECoG) [44].

The patients stayed in the hospital implanted for 7 to 10 days, during which we can record physiological data after having obtained consent.

Neurophysiological data were recorded using Natus (Pleasanton, CA) and the sampling rate was 2048 Hz. For each experiment, we got a TTL file containing the SEEG recordings from the hospital.

### 3.1.2 Experimental Design and recordings

Participants were seated in their hospital bed brought to a semi lying position in front of a board placed on the bed table The board consisted in a 40.8cmx40.8cmx1.3cm and made of Plexiglas. We made sure that the patient was at a correct distant allowing him to reach comfortably the objects. The board was equipped with three types of objects of different size and shape and a hand resting plate. Four touch sensors (AT42QT1011, SparkFun Electronis, Niwot, CO, USA) were implemented under the three objects and the hand resting plate and 3 LED were placed next to each object. The touch sensors had a built in 1nF capacitors. This allowed the sensors to be sensitive enough to detect when the objects were grabbed but not too sensitive that the mere placing of the objects could trigger a

signal (1).

Different shapes and sizes were used to induce different types of grip: power grip (cylinder of 6.35cm diameter and 3.81 cm height), prehension grip (thin disk of 5.54cm diameter and 2.36cm height) and precision grip (small cylinder of 1.113cm diameter and 7.56mm height). The two objects for power and prehension grip were covered with a cupper band to allow conduction whereas the object used for precision grip was made directly of cupper. The sensors

and lights were connected to the computer via a 12-bit data acquisition board (USB-1208FS, Measurement Computing Corporation, Norton, MA, USA) and controlled by custom scripts in matlab using the psychophysics toolbox [45]. This experimental setup is designed to ensure naturalistic conditions (i.e., a real person performing actions instead of video stimuli) while measuring all the characteristics of executed and observed actions.
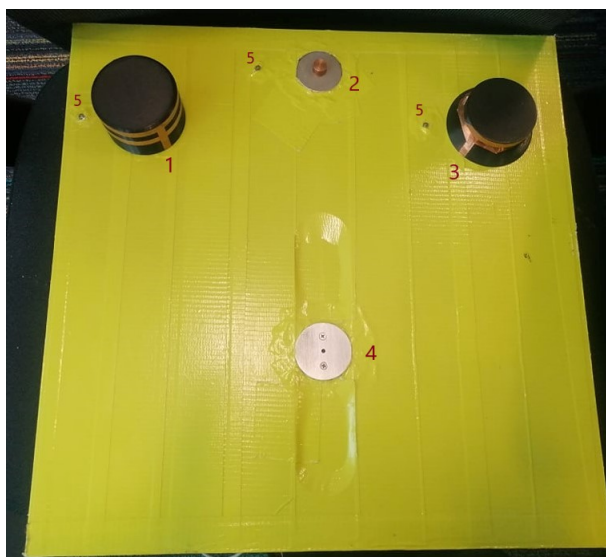


Figure 1: Picture of the board used for experiments. (1) corresponds to power grip, (2) to precision grip and (3) is prehension grip. (4) is the hand resting plate whereas (5) are the LED.)

During the action execution phase, the patient would keep his hand on the hand resting plate while waiting for the cue. The cue happens between 1.5 and 2 seconds after the beginning of the trial and consisted of a sound (sampling rate of 48kHz) that last between 1.5 and 2.5 seconds (SoundOn) and a LED (cueOn) that would light up for 500ms indicating which object to grab. Once the sound was stopped (soundOff), the pa-

tient could, at his own pace, lift his hand from the hand resting plate (HandOut), reach for the object (objTouch), release the object (objRelease) and put his hand back on the hand resting plate (handBack). Once the hand is back on the resting plate, we wait for 250ms and we go on with the next trial (2).
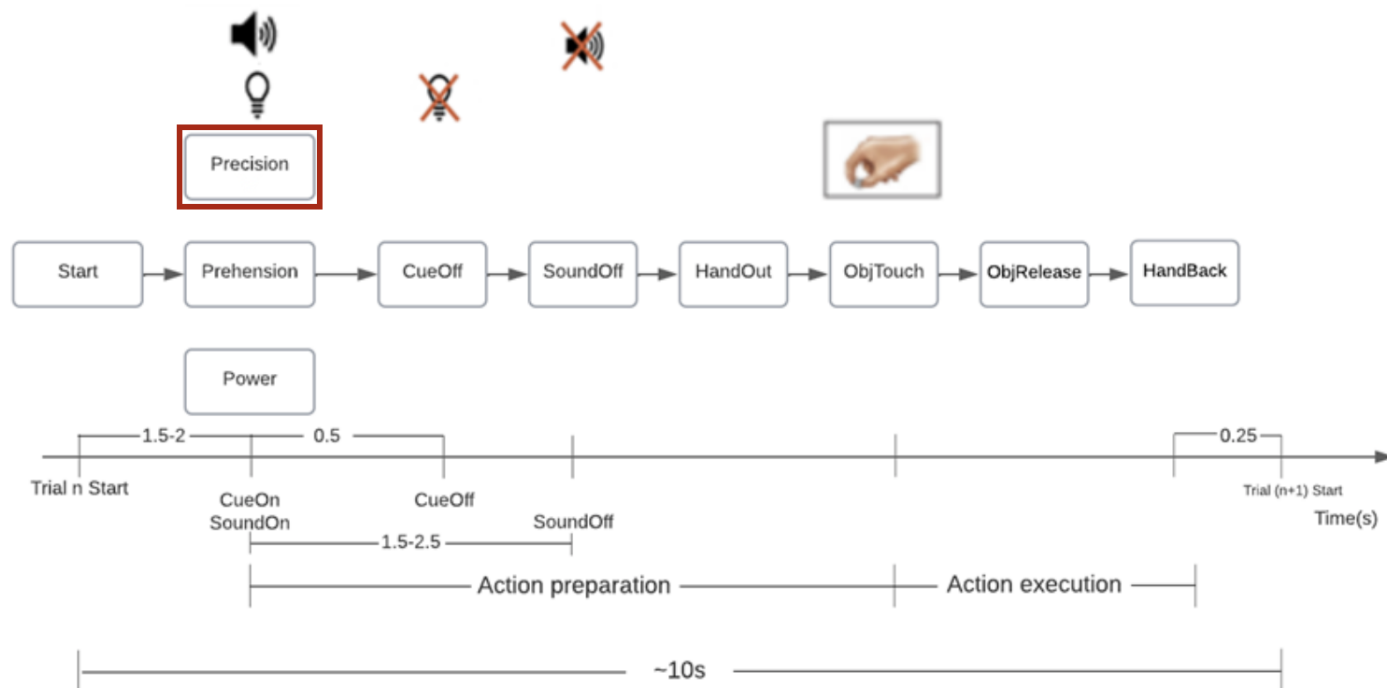
Figure 2: The panel shows the unfolding in time of the experimental design. At each trial, the participant is cued by a light to perform an action (here, precision grip) and is required to perform it when another cue (a sound) is turned off.

During the observation phase of the experiment, the patient was asked to carefully watch the experimenter perform the task described above. The experimenter was sited in front of the patient because this is what best reflects how we most often perceive other's movements in real life

So as to keep the experiment more entertaining for the patient, we divided the experiment into smaller blocks and alternated between execution and observation phases. Each phase would stop once we reached n correct trials for each object (n being the same for each object). The experiment lasted for as many blocks as the patients felt comfortable doing.

In total, each trial unfolds as follow:
Wait in start position (1.5-2s), SoundOn (1.5-2.5s), Action Execution (4-6s, depending on the patient's pace), wait until mext trial (250ms). Therefore, we estimated that each trial lasts approximately 10 seconds (2). As there are three types of objects (prehension, precision, power

grip) and two phases (Action execution and Observation), in total there are 3 x 2 = 6 conditions. If we want to have 15 correct trials per condition if would take at least 10s x 30 trials x 6 conditions = 900s = 15min, that is considering a 100 percent success rate, meaning that the patient perform each trial correctly. If we consider that the patient has a 30 percent success rate (which is rational considering that the patients are often worn out from surgery), then it would take almost 50 minutes to obtain 15 correct trials per condition, which is a reasonable amount of time to spend with the patient.
We set a maximal duration of 20 seconds per trial, if the patient did not finish the task in that time limit, the trial is aborted and we move on to the next one.

For each block, we recorded the timing of every event on a matlab file (8) (unfortunately, due to an error in the code, the event 'HandOut' was not recorded for the last patient, but this

error has been corrected since). Additionally, we recorded other parameters necessary for further analysis. First, we needed to send several triggers to allow us to align these matlab files with the SEEG recordings (TTL file). The triggers that we sent was as follow:

A long trigger at the beginning of each block, the trigger would last 300ms if the block was an execution trial and 400ms if it was an observation one.

We also added three triggers at the beginning of each block that will act as a time-coded unique identifier to differentiate each blocks and be able to link each matlab file with the correct block on the TTL file.

Then, we send triggers that were multiples of 30ms for : TrialStart (30ms), cueOn (60ms), objTouch (90ms) and HandBack (120ms). A trigger was also sent if the patient touched the wrong object (20ms).

The timing of each trigger is saved in the matlab file (8).

When sending a trigger, there can be a small delay between the moment we send the trigger (which will be saved on the computer) and the moment it is actually recorded. This delay depends on the computer used for the experiment. Therefore, calibration tests needed to be done with a multimeter to estimate the delay induced by my laptop.

We implemented a discard key used to discard the trials that were wrongly executed due to external factors that cannot be recorded directly on the computer (for example if a parent or a nurse comes in and talks to the patient during the trial). This key is especially useful during the observation phase where we need to make absolutely sure that the patient is paying attention to what the experimenter is doing. The discard key is controlled via the keyboard. If any key on the keyboard (except for the space bar and the sound buttons) is pressed at anytime during the trial, then the discard key for this trial takes the value 1, otherwise it stays at 0. The value of the discard key is saved on the matlab file at every trial.

The space bar is used for pausing the program

if needed, if the patient is getting tired or did not understand the task properly and need to be explained again or to take some rest. The sound buttons are used to adjust the volume so the patient can hear the beeping cue properly.

Finally, there is a last parameter saved in the matlab file called "error_code". Indeed, several errors can occur during the trial. The mistakes that we though could happen were:

-grabbing the wrong object,

-be too slow and exceed the maximal duration of 20 seconds,

-premature arm movement during "sound cue" without waiting for the end of the cue (meaning the patient would move his arm between SoundOn and SoundOff),

-not keeping his hand on the hand resting plate between the beginning of the trial and the beginning of the cue.

If the trial was carried out correctly, the error_code parameter takes the value 0, otherwise it takes a different value (-1, 1, 2 or 4) depending on which of the previousy mentioned error has occured. If any other error that was not listed above happens, the experiment can press the discard key to record this trial as incorrect.

Table (8) in annex is a summary of all the paramaters saved during the experiment (throughout the rest of this report, I will used the abbreviations that are detailed in this table).

### 3.1.3 Discussion about the experimental design

The parameters described above are the latest version, but they have been adjusted over time. We made a few changes after each patients in order to respond to some problematic points that have been raised.

During the first two experiments, there was no sound being played. The only cue was the LED that would light up for a duration between 1 and 2 seconds. The patient was asked to wait until the LED was off to go and grab the object. The objective is to study what happens in this period of time where the patient knows what the movement is going to be next, without doing it. However, the main problem that

occured was that the patient would not wait for the LED to go off before grabbing the object, resulting in an error (premature arm movement during cue presentation). To solve this problem, we implemented the sound that would play for a random duration between 1.5 and 2.5 seconds while the LED only stays on for 500ms. That way, we still have this time interval (between cueOff and SoundOff) where the patient knows what object will be grabbed while the movement is still not initiated. We thought that it would be easier for the patient to wait until the end of the beep sound instead of the light. This worked well as we did not get any error due to premature arm movement with the third patient.

In the version of the experiment used with the first two patients, we were sending 8 short triggers of 15ms at the beginning of each block, 3 triggers of 25ms at trialStart, 1 trigger of 25ms for cueOn and 1 trigger of 25ms for objTouch. When aligning the matlab files with the SEEG recordings for these patients, we realized that having triggers of the same duration for each event involved a complex analysis. We also had no way of distinguishing between each block and had to do it manually. Moreover, we couldn't distinguish a correct trial from a trial where the patient touched the wrong object on the TTL file. That is why we decided to add triggers at the beginning of each block to tell each block appart and differentiate between execution and observation phases. We also added a trigger for wrong object and made the triggers for each event of different lengths.
In the prior versions, we also did not have any way to pause the experiment or to discard the trials. We realized during the first experiments that the patient can easily be disturbed or loose focus, especially during the observation phase . That is why we added the discard key and a way to pause the experiment.

In the previous models of the experiment, each block would stop when we reached 3xn number of trials (n being the number of trials per object). However, these trials were not necessarily correctly carried out. Therefore, we could end up with only a very few number of correct trials that can be used or with an unequal distribution of correct trials between each type of object. To correct that, we made sure that the block stops when we reach n correct trials for each object.

Finally, we wondered if the distance between the three objects could impact the response that we will obtain for the different grips. Indeed, if after analysis we find a significant different response between grips, the question could be raised that it is not necessarily due to the different movements that were performed but because the objects are in different field of views, leading to different visual stimuli. We considered switching the three objects for a single one that would combine the three grips. The cue would then be either a LED that lights up in different colors (one color for each grip), or three different types of sound (each sound indicating one type of grip). Ultimately, we decided that this solution would be too complicated and confusing for the patient. To remedy this problem, we decided to switch the position of the objects from times to times.

### 3.1.4 Summary of experiments conducted

During the experiment with the first patient, we started with the execution phase. We ran a first block with 30 trials (10 for each object). The patient was often too fast (meaning grasping the object before the end of the cue, resulting in the error 'premature arm movement') or too slow (going the object after the end of the maximal time), and often forgot to put the hand back on the resting plate. The patient was also easily losing concentration and had to be reminded how the task worked regularly. We winded up with only 2 correct trials out of the 30. During the second execution block,the patient felt tired during the experiment so we stopped after 12 trials and again, we only had 2 correct trials out of the 12. As for the observation phase, we ran 15 trials (5 for each object) but the patient was

easily disturbed and not paying strong attention.

For the second experiment ran, the patient had autism, behavioral issues, lack of impulse control and was proned to hallucinations. During the execution phase, the main issue was that the patient was not waiting for the LED to turn off before going for the object, which could be due to the lack of impulse control previously mentioned. The second issue was that the subject had trouble really grasping the object and was just slightly touching it (even though being frequently reminded to truly grab it). Therefore it was not detected by the touch sensor. This is probably because the patient was sleep deprived and therefore really tired. We ran 3 experiments with 10 trials for each object, so 90 trials in total and obtained 14 correct trials. Regarding the observation phase, it was really difficult to keep the patient focused. The subject was very disturbed by a balloon in the hallway which was probably causing some hallucinations. Therefore, I did not performed a lot of observation trials, only 1 experiment with 5 trials for each object (15 total) during which the patient was not really focus.

However, for the third patient we performed 4 blocks, 1 observation phase with 10 correct trials for each object, 1 execution phase with 15 correct trials for each object, another observation phase with 10 correct trials for each condition and a last execution phase with 15 correct trials for each condition.
In total, for the observation phase, we have 20 correct trials for each object (60 trials in total). The patient was very focus. To make sure that attention was being payed, I paused the experiment several times to ask what object I just touched, and the patient gave the correct answer each time. I didn't have to discard any trial.

For the execution task, we got 30 correct trials for each condition (90 correct trials and 127 trials in total, so approximately 70% of correct trials). The patient was feeling good, did not seem tired. We just had to pause the experiment twice to remind the patient to wait until the end of the sound to grab the object but otherwise the experiment was performed well. There were no external distraction and no trial were discarded.

There were no seizure events in any of the sessions for any of the patient.

In light of these results, we ran the data analysis with the data collected with the third patient only.

### 3.1.5 Electrode reconstruction

The patient had 15 stereoelectroencephalography (SEEG) electrodes (PMT Corporation, Chanhassen, MN, USA). The electrodes' diameter was 0.8 mm and contained 8–16 contacts (the contacts were made of platinum, 2mm length and the center to center contact spacing was 3.5mm) (see Figure 18 in Annex). To do this electrode reconstruction, we needed the implantation map (Figure 3), the characteristics for each electrode (Figures 17, 18 in Annex) MRI and CT scans of the patient, which have been provided to us by the Boston Children's Hospital. We used the iELVis (Groppe et al., 2017) pipeline to localize the depth electrodes. The pre-surgical MRI scans was processed and automatically segmented by Freesurfer (Dale et al., 1999; Reuter et al., 2012), followed by co-registering the post-surgical CT to the processed MR images. Electrodes were then identified visually and marked in each subject's co-registered space using the BioImage Suite (Joshi et al., 2011). Each electrode was assigned an anatomical location using the Freesurfer localization tool.

Figures 4, 5 and Table 2 report the distribution of electrode locations.
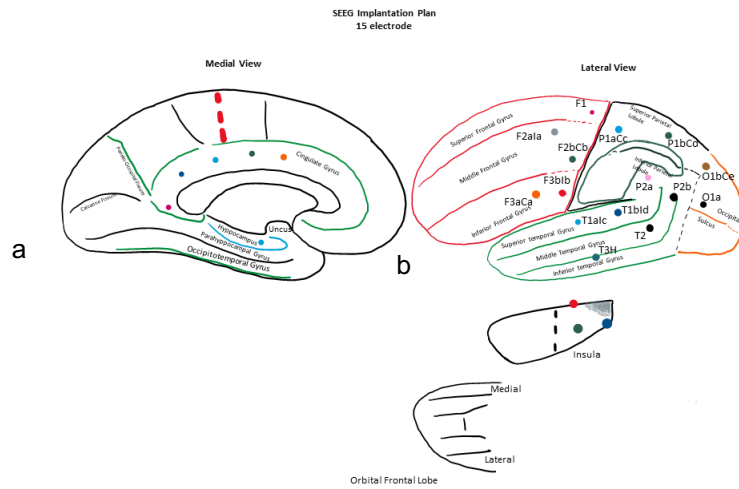
Figure 3: SEEG implantation plan shown with left medial (A) and left lateral (B) views. The patient was implanted with 15 electrodes with 6 to 16 channels each.
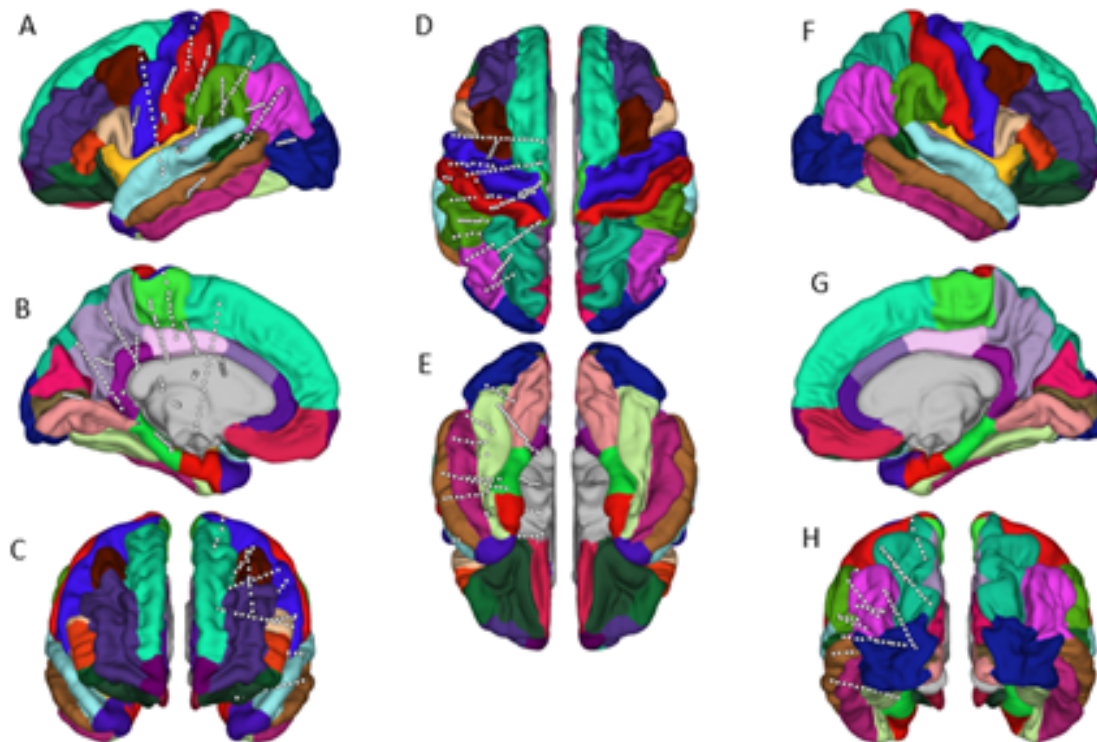


Figure 4: Electrode locations on the average brain atlas. Location of all n=160 electrodes shown with different views. A: Left lateral; B: Left medial; C:Anterior; D: Superior, whole brain; E: Inferior, whole brain; F: Right lateral; G: Right medial; H:Posterior
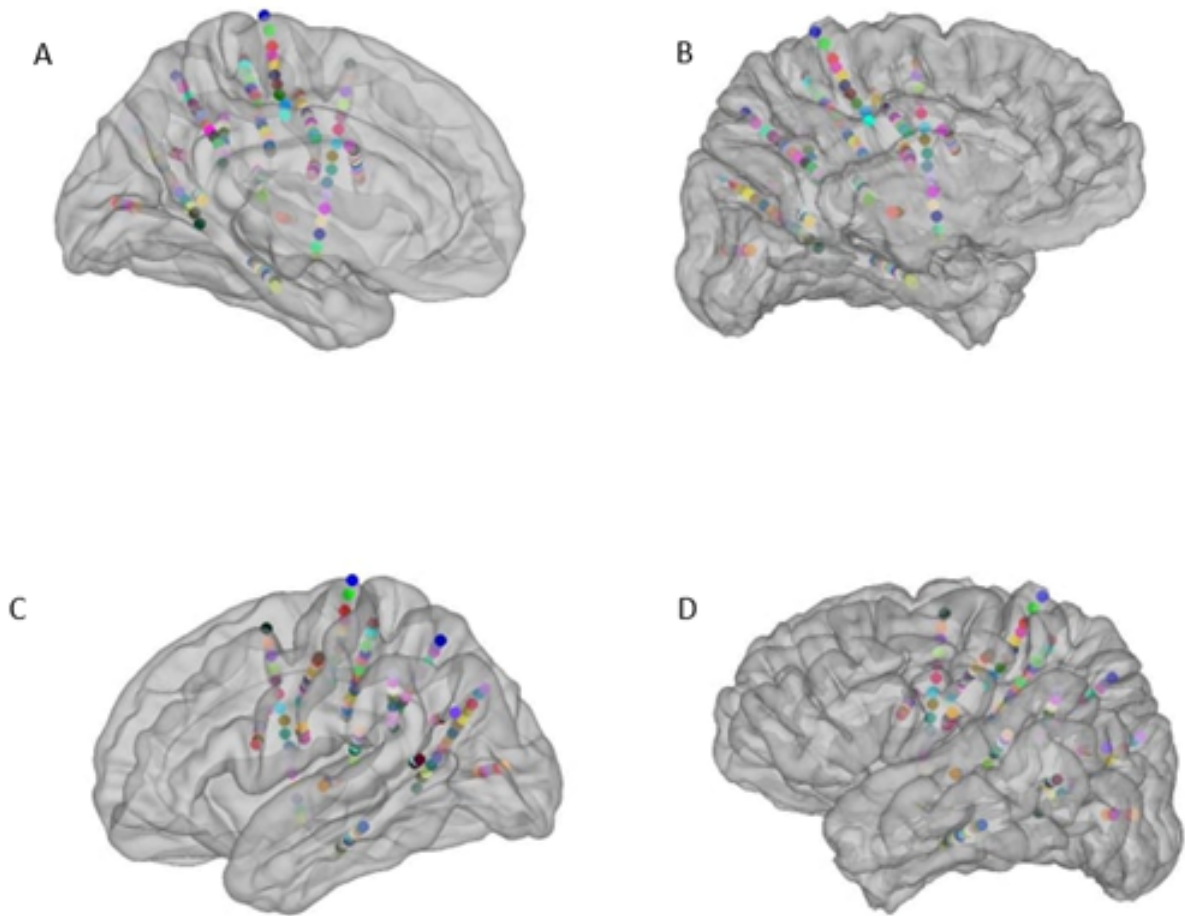
Figure 5: Electrode locations. Location of all n=160 electrodes overlayed on the Desikan Killiany Atlas shown with different views. A: Right lateral; B: Left medial; C: Left lateral; D:Right Medial

| Location | Count | Channels name |
|---|---|---|
| Left-Cerebral-White-Matter | 105 | O1a1, O1a2, O1a3, P2b1, T21, T22, T23, T26, T3H1, T3H2, T3H3, T3H4, T3H5, T3H6, T3H7, T3H8, T3H9, T3H10, T3H11, T3H12, T1aIc4, T1aIc5, T1aIc6,T1aIc7, T1aIc8, F3aCa3, F3aCa4, F3aCa5, F3aCa6, F3aCa7, F3aCa8, F3aCa9, F3aCa10, F3aCa11, F3aCa14, F3aCa15, F3aCa16,F3bIb1, F3bIb3, F3bIb4, T1bId1,T1bId2, T1bId3, T1bId5, T1bId8, T1bId9, F2bCb2, F2bCb3, F2bCb4, F2bCb5, F2bCb6, F2bCb7,F2bCb8,F2bCb9, F2bCb10, F2bCb14, P2a1, P2a2, P2a3, P2a4, P2a5, P2a6, P2a7, P2a8, O1bCe4, O1bCe5, O1bCe6, O1bCe7, O1bCe8, O1bCe9, O1bCe10, O1bCe11, O1bCe12, O1bCe13, O1bCe14, P1bCd3, P1bCd5,P1bCd6,P1bCd7, P1bCd8, P1aCc2, P1aCc3, P1aCc4, P1aCc7, P1aCc8, P1aCc12,P1aCc13,P1aCc14, F15, F16, F17, F18, F19, F2aIa1,F2aIa2, F2aIa3, F2aIa4, F2aIa5,F2aIa6, F2aIa8, F2aIa9, F2aIa10 F2aIa12, F2aIa13, F2aIa14 |
| ctx-lh-precentral | 3 | F2aIa11, F2aIa15, F2aIa16 |
| ctx-lh-insula | 4 | T1aIc1, T1aIc2, F3bIb2, F2aIa7 |
| ctx-lh-postcentral | 8 | F3bIb5, F3bIb6, F3bIb7, F3bIb8, F2bCb11, F2bCb12, F2bCb13, F110 |
| ctx-lh-paracentral | 4 | P1aCc6, F12, F13, F14 |
| ctx-lh-posteriorcingulate | 5 | F3aCa1, F3aCa2, F2bCb1, P1aCc1, P1aCc5 |
| ctx-lh-superiorparietal | 7 | P1bCd9, P1bCd10, P1bCd11, P1bCd12, P1aCc9, P1aCc10, P1aCc11 |
| ctx-lh-precuneus | 1 | P1bCd4 |
| ctx-lh-isthmuscingulate | 4 | O1bCe2, O1bCe3, P1bCd1, P1bCd2 |
| ctx-lh-lingual | 1 | O1bCe1 |
| ctx-lh-inferiorparietal | 7 | P2b2, P2b3, P2b4, P2b5, P2b6, T24, T25 |
| ctx-lh-parsopercularis | 2 | F3aCa12, F3aCa13 |
| ctx-lh-transversetemporal | 1 | T1aIc3 |
| ctx-lh-lateraloccipital | 2 | O1a4, O1a5 |
| ctx-lh-superiortemporal | 3 | T1bId4, T1bId6, T1bId7 |
| unknown | 3 | O1a6, F11, T1bId10 |

Table 1: Distribution of electrode locations. Number and name of channels for each location. Channel 1 corresponds to the deepest channel.

| Electrode | Number of channels |
|:---------:|:------------------:|
| F1 | 10 |
| F2aIa | 16 |
| F2bCb | 14 |
| F3bIb | 8 |
| F3aCa | 16 |
| T1aIc | 8 |
| T1bId | 10 |
| T3H | 12 |
| T2 | 6 |
| P2a | 8 |
| P2b | 6 |
| O1a | 6 |
| O1bCe | 14 |
| P1aCc | 14 |
| P1bCb | 12 |

Table 2: Number of channels for each electrode. Channel 1 corresponds to the deepest channel.

## 3.2 Data Analysis

### 3.2.1 Data preprocessing

To perform this data analysis we used the Chronux Toolbox on Matlab (Mathworks, Natick, MA, USA, version R2021a) [46]. The data was collected in EDF (European Data Format). The very first step was to convert them into a matlab file and to extract all the channels. Once this was done, we preprocessed the data by applying a bandpass filter (second-order bandpass filter between 1 and 100Hz) and a notch filter at 60Hz (Matlab function "filtfilt") to remove the AC line frequency.

The following step was to align our matlab files with the triggers sent in the TTL file. Once this alignment was done, we only kept the correct trials (the one that were completed with no error and were not discarded by the experimenter). For each condition, trial and channel, the signal was aligned with each event (HandOn, CueOn, SoundOff, ObjTouch, ObjRelease, HandBack).

We then checked for artifacts, outliners and abnormally distributed trials and remove them. To detect artifacts we computed the range (difference between maximun and minimum value) for each trials. We considered as artifacts the trials whose range were over three times the standard deviation away from the mean range across trials.

The abnormally ditributed trials were the ones whose kurtosis differs more then 2 standard deviations from the mean kurtosis across trials .

Finally, the ouliners were the trials that had an absolute mean value over three times the standard deviation from the absolute mean across trials in the same interval. We only remove the trials from the electrodes where they were detect as abnormal, but we keep the rest of the channels.

Table 3 shows the number and percentage of remaining trials (across all 160 electrodes) used for further analysis. As a reminder, for this patient we performed two blocks for execution task with 15 correct trials per object for each, so we have 30 trials per object for motor task, and 2 blocks for observation task with 10 correct trials per object, so 20 trials per object for vusual task. Multiply by the number of channels (160), this is 3200 for perception task and 4800 for execution task. The number of trials removed is balanced between gip types so we still have an equal distribution of trials across grip types.

14

|  | Prehension Grip | Precision Grip | Power Grip |
|---|---|---|---|
| Action execution | 4725 (98.44%) | 4722(98.37%) | 4684(97.58%) |
| Action perception | 3171(99.09%) | 3152(98.5%) | 3160(98.75%) |

Table 3: Number and percentage of trials remaining across all 160 channels after removal of artifacts, outliners and abnormally distributed trials.

### 3.2.2   Time-frequency analysis

Once the data were retrieved, aligned and filtered, we wanted to give us an idea of which frequency bands contain important informations for executions and observations tasks. To do so, we investigated the power of the IFPs versus time for each electrodes, both conditions and each object. We calculated the power spectra of the IFP using a multi taper time-frequency analysis with a time-bandwith product (TW) of 3, 5 tapers (the number of tapers used must be less than or equal to 2TW-1), a window size of 0.3s and a step size of 0.01s was computed. Each trial was divided by the baseline, which was defined for each trial as the interval of -0.1s and 0.1s around cueOn. We chose this baseline after inspection of the spectrograms and IFPs as it was the interval where it did not seem to have any activity. At first we chose an interval of -200s to 0s before cueOn in a way to not have event happening in the interval, but it looked like there was some residual neuronal activity from the previous trials. After realising that, we increased the HandRestTime (time between the beginning of the trial and cueOn) to be able to take an interval for the baseline of 200ms before cueOn without having residual activity from previous trials. Unfortunately, we did not have any other patients after doing this modification. For each channel, we plotted the spectrograms for every trial, as well as the average over trials and for both conditions.

We plotted the spectograms in a frequency range of 1 to 100Hz.

### 3.2.3   Electrodes selection

Once we got an idea of the frequency bands that encoded interesting information, we wanted to determine which electrode and channel gave significant responses in those ranges. To do that,

we were inspired by the method detailed by Anat Perry et al. in their paper published in 2017 [47]. We first band-pass filtered the signal in the frequency ranges we deemed interesting (3.2.2) and a Hilbert transform was applied for each trial per electrode, per object and per condition. The advantage of using the Hilbert transform instead of the IFPs is that the Hilbert transforms eliminate the negative frequency part and double the magnitude of positive frequency part in order to keep the same power but work only with positive components. Therefore, if a negative drop happens right after a positive peak, we will record them both, when we would have get an average of zero if working with IFPs. This is especially interesting in our case where our trials are not perfectly aligned (each event is performed at the patient's pace and varies between trials). Then we applied the matlab function "smoothdata" to average each sample of the signal with its neighbors (we chose a window of 0.5ms). To identify periods of significant activation for each channel, two-sample t-tests (alpha levels set at 0.05, using the matlab function "ttest2") were performed, comparing each sample of the hilbert transform (averaged across neighbors) with the baseline (chosen as explained in section 3.2.2) for each electrode per condition and per object. We considered as significatively responsive, the channels that showed at least 300 ms of consecutive significant signal (we took a treshold of -10logpvalue $\geq$ 2). From these electrodes, we focused primarily on the ones that were not in the white matter ad that were responsive for both conditions.

### 3.2.4   Integrated power

In order to focus more precisely on certain observations made with the spectrograms, we plotted the temporal evolution of the integrated

15

power in specific frequency ranges (0.1 Hz to 7 Hz, 8 Hz to 15 Hz, 15 Hz to 25 Hz, and 45 Hz to 70 Hz) for each conditions (visual and motor task) and for each channel that was deemed interesting by the method described in section 3.2.3. The signals were averaged across trials and objects.

For a purpose of assessing the differences between condition and grip types, we plotted the integrated power over time in the same frequency ranges for each conditions and for each object, averaged across trials.

### 3.2.5 Statistical analysis to evaluate the difference between condition and the ability to distinguish between grip types

We wanted to evaluate if there was a significant difference in power modulation between motor and visual taks around specific event, frequency range and electrode. To do so, we computed the average power in a time-frequency rectangle for each condition (execution or observation), and each significant electrode. This gave us a vector of one value per trial for each condition that we compared with the vector for the other condition using Student's unpaired t-test

($\alpha$ level=0.05), the null hypothesis being that the average across trials for one condition is the same as the average across trials for the other. We performed these t-test for several time intervals, in particular in intervals of 0.5s around cueOn, soundOff, ObjTouch and ObjRelease. As both conditions had different number of trials to increase the power of the t-tes we took the first 20 trials for motor task in order to have same-size samples.

Finally, we also wanted to estimate in which frequency range and which electrode was able to distinguisgh between grip types. Similarly as before, the average power in a time-frequency rectangle was taken for each condition and each significant electrode. We ended up with a vector of one value per trial for each grip type that we compared with the vector for another grip type using Student's unpaired t-test ($\alpha$ level=0.05), the null hypothesis being that the average across trials for one grip type is the same as the average across trials for another grip type. We performed these t-test for the same time intervals as previously. As we have three different object, each condition and electrode has three comparison ttest. In the end, each electrode for each object gets a "differentation result" that can go from 0 to 3 based on the number of significant t-tests.

# 4   Results

## 4.1   Time frequency analysis

In order to get a sense of which frequency ranges carry major information with regards to action execution and action observation, we performed a multi taper time-frequency analysis for every channels (160 in total) for frequencies between 1 et 100 Hz.

Figure 16 shows the modulation from baseline (defined as -100ms to 100ms around cue cue) for both conditions for three channels of electrode F3aCa, located in the inferior frontal gyrus. Channel FaCa2 is the deepest one, while FaCa8 is the most superficial one. FaCa2 is located in ctx-lh-poseriorcingulate and both FaCa6 and FaCa8 are located in the left-cerebral white matter. We decided to present the spectrograms from this electrode after inspection of the IFPs and of all spectrograms, as it was the one that showed the best responses (see Figure 16 in Annex).

From these spectrograms, we can directly see that the responses seem to be condition and depth-dependant. The responses do not appear to differ between grip type for the motor task but there seems to differ for observation tasks.

During motor task, we can observe at least two discernable changes with respect to baseline.

An increase in power compare to baseline can be detected in a low and mid frequency range (0.1 Hz to 20 Hz) and in the high frequency band (45Hz to 70Hz).

If this second power increase in the gamma band is visible for the three channels, the increase in power in the low and mid frequency bands is only present for channel FaCa6. The increase in the $\delta$-delta, $\theta$-theta and $\alpha$—alpha bands are present specifically between SoundOff and ObjTouch and between ObjRelease and Handback, so during movement. The power increase in higher frequency bands however is broader and starts a little before SoundOff and extends shortly after HandBack.

For the observation task, the responses are much weaker but seems to behave similarly. Indeed, we can still distinguish small increase in power with respect to baseline in the low and mid frequency bands (from 0.1Hz to 20Hz) and in the high frequency band (between 45Hz and 70Hz) for channel FaCa6 even though no clear pattern seems to emerge. However, the patches in high frequency band are present only for prehension and power grip, especially the power grip that evoke a stronger increase in power than the preension grip.

17
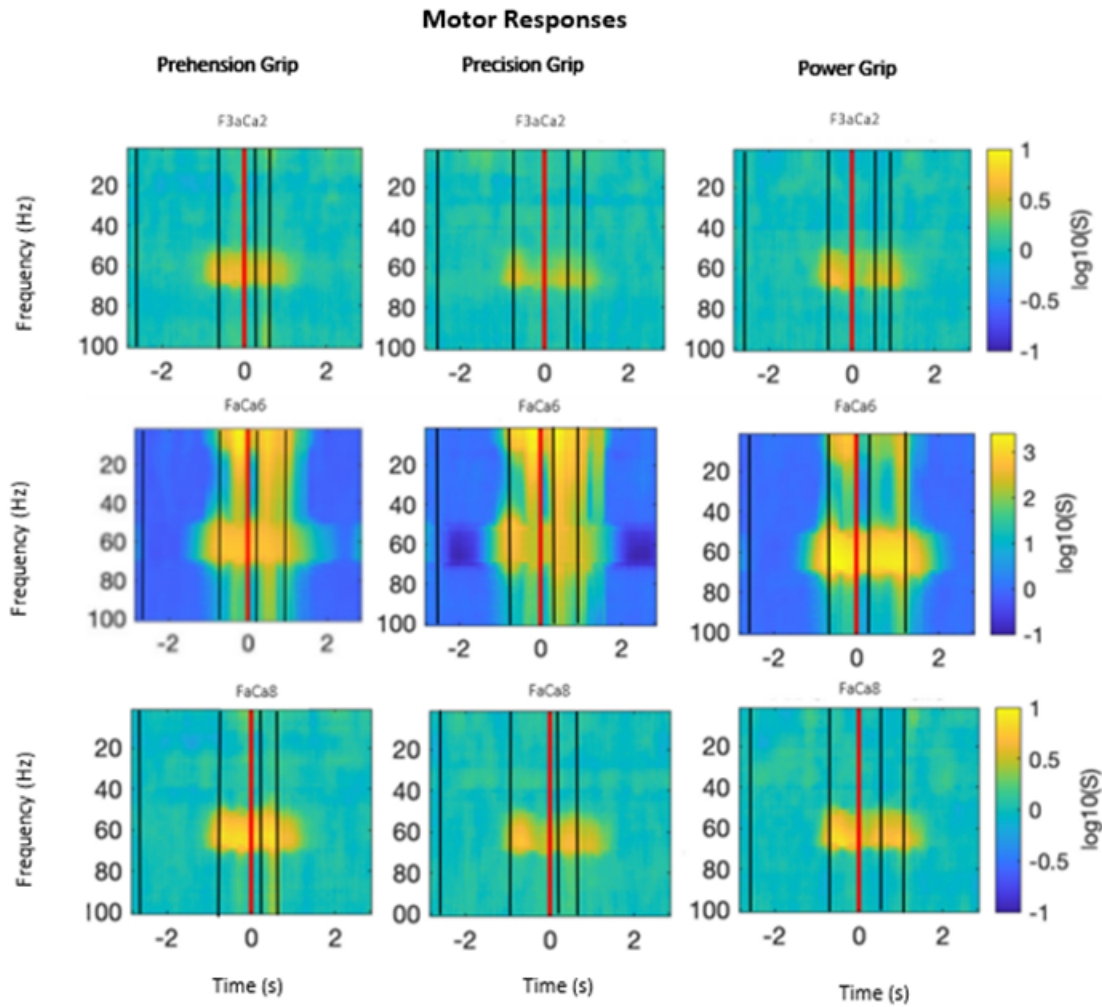
Figure 6: Time-frequency analysis of the motor responses from 3 channels of electrode F3aCa located in the inferior frontal gyrus, averaged across all trials, for all three objects. From top to bottom row, the channels go from deepest to most superficial. The tasks were aligned with ObjTouch (t=0 and the vertical red lines correspond to the average time of the occurrence of this event). The vertical black lines correspond to the average time of the occurrence of the events (from left to right): CueOn, SoundOff, ObjRelease and HandBack.
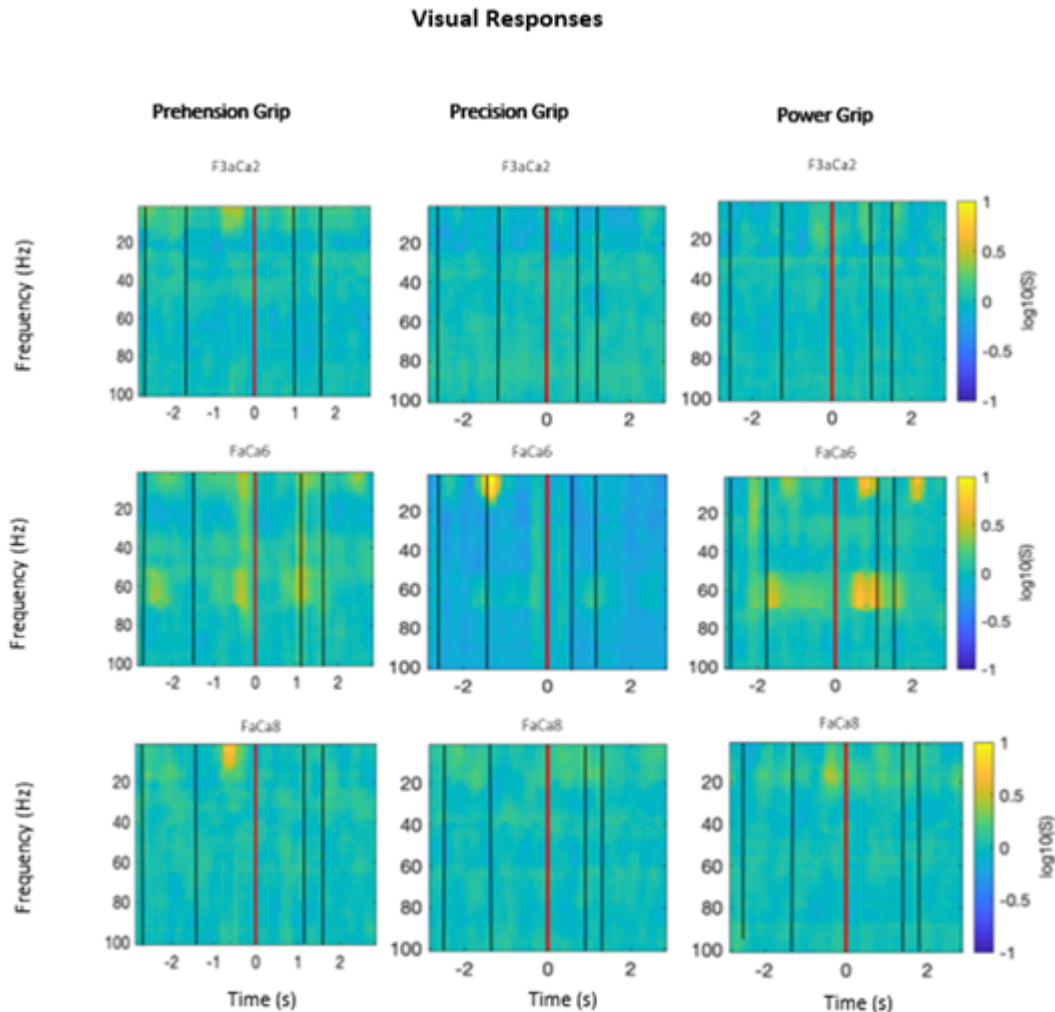
**Visual Responses**



Figure 7: Time-frequency analysis of the visual responses from 3 channels of electrode F3aCa located in the inferior frontal gyrus, averaged across all trials, for all three objects. From top to bottom row, the channels go from deepest to most superficial. The tasks were aligned with ObjTouch (t=0 and the vertical red lines correspond to the average time of the occurrence of this event). The vertical black lines correspond to the average time of the occurrence of the events (from left to right): CueOn, SoundOff, ObjRelease and HandBack.

With these spectrograms we could identify frequency bands that seems to hold interesting informations. We also saw that the responses differ between motor and visual responses but also between channel depth. However, it didn't seem to be a difference between grip type. In the following section, done to confirm or refute that, which is what we did in the following section.

## 4.2 Integrated Power in different frequency bands

The goal of the next step was to zoom in the different frequency ranges that appeared to encode interesting information from the spectrograms and study more in details the observations that were ade by visual inspection of the spectrograms. Based on the results of the spectrograms, but also based on the literature (see section 2.2), we decided to focus on 4 frequency bands : from

19

0.1 to 7Hz ($\delta$—delta and $\theta$—theta bands), from 8 to 15Hz ( $\alpha$-alpha band), 15 to 25Hz($\beta$-beta band) and 45 to 70Hz ($\gamma$-gamma band).

Table 4 summarizes the electrodes that were found reponsives using the method described in section 3.2.3 in this different frequency bands. We found more significantly responsive elec-trodes for motor task ( 20%) than for observation task ( 5%), which was expected as most of the electrodes are on the frontal lobe, which contains the motor cortex. We focused only on the electrodes that were responsive for both conditions and located in the grey matter.

| Frequency Range (Hz) | Electrode | Location | Condition | Grip type |
|---|---|---|---|---|
| [0.1 7] | T1aIc3 | ctx-lh-transversetemporal | 1 | 2 |
| | | | 2 | 3 |
| | O1bCe3 | ctx-lh-isthmuscingulate | 1 | 2 |
| | | | 2 | 2 |
| [8 15] | T1bId6 | ctx-lh-superiortemporal | 1 | 1-2-3 |
| | | | 2 | 3 |
| | F3bIb7 | ctx-lh-postcentral | 1 | 1-2-3 |
| | | | 2 | 2 |
| | O1a4 | ctx-lh-lateraloccipital | 1 | 1 |
| | | | 2 | 2 |
| [15 25] | F3bIb7 | ctx-lh-postcentral | 1 | 1-3 |
| | | | 2 | 2 |
| | F1*2 | ctx-lh-paracentral | 1 | 1-2-3 |
| | | | 2 | 3 |
| [45 70] | P1aCc9 | ctx-lh-superiorparietal | 1 | 1 |
| | | | 2 | 1 |
| | F2aIa16 | ctx-lh-precentral | 1 | 2 |
| | | | 2 | 3 |

Table 4: Electrodes with significant responses (-logpvalue of the ttest comparing each sample to the baseline of the hilbert transform $\geq 2$ for at least 300ms consecutive) and their location, by condition (1=motor task, 2=observation taks) and grip type(1=prehension grip, 2=precision grip and 3=power grip).

### 4.2.1 Integrated Power vs. condition

From inspection of the spectrograms, we saw that the responses differed between visual and motor tasks. Both seem to give response in the high frequency range (45 to 70Hz) and in low-mid frequency range (between 0.1 and 15Hz) but the visual responses were weaker than motor responses, especially in the high frequency band. To further study this, the temporal evolution of the average power for execution and observation tasks were plotted in different frequency ranges. Figures 8, 9, 10 and 11 show the results recorded from the significant channels (as shown in Table 4). Trials were aligned with ObjTouch (red line in top left picture).

Visual and motor responses behave similarly but the visual responses are weaker, which agrees with our observations form the spectrograms. We can distinguish two increases in power, the first one, which is the strongest one, starts after cueOn and reached its peak at SoundOff, then it decreases until ObjTouch and increases again to a lower level at ObjRelease until HandBack (Figure 11). Both visual and motor responses show the same dynamic witht he peaks being synchronized.

Similar behavior is observed in the low and

mid frequency range as well. There are two discernable pics around SoundOff and ObjRelease (Figures 8 and 9). However, for electrodes T1bId6, O1a4, T1aIc3 and O1bCe3, it appears that the visual responses are stronger than the motor ones (Figures 9a, 9c, 8a and 8b).

Interestingly enough, in the frequency range of 15 to 25Hz, for motor tasks, we can observe an increase in power before CueOn, followed by a big drop of power happening during movement until ObjRelease (Figure 10). For visual tasks, we can see a small decrease after SoundOff (at the onset of movement), quickly followed by an increase in power.
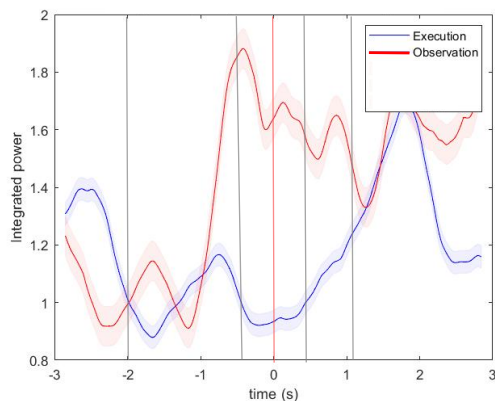


(a) Channel T1aIc3
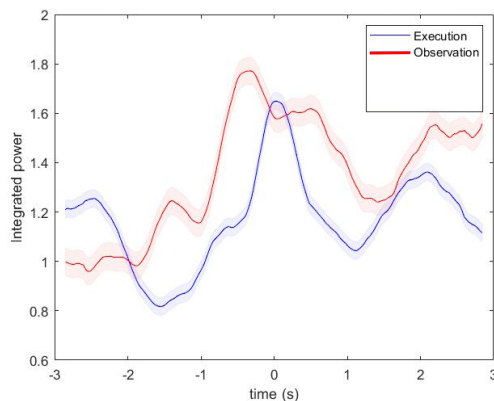
(b) Channel O1bCe3

Figure 8: Average power recorded by the significant electrodes in frequency band 0.1 Hz to 7 Hz with respect to the baseline for execution and observation tasks. The shades represent the standard deviation. Trials are aligned with ObjTouch (red vertical line on top left picture). The black vertical lines on top left picture are, from left to right: cueOn, SoundOff, ObjRelease, HandBack.
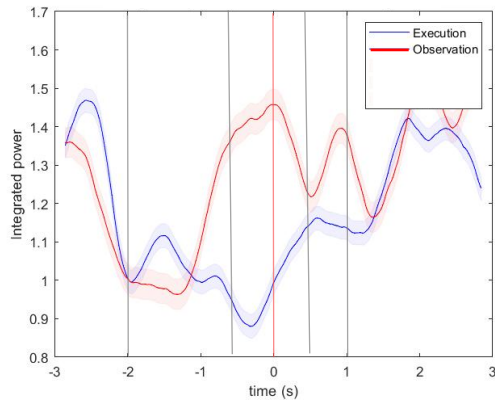
(a) Channel T1bId6
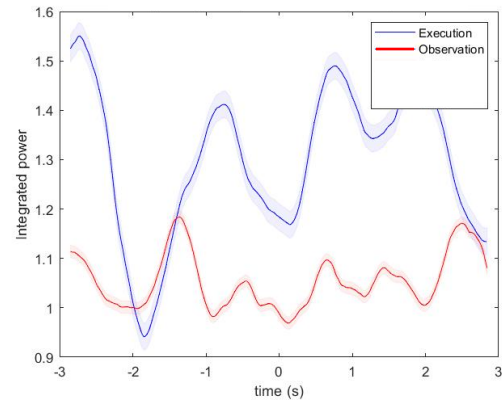
(b) Channel F3bIb7
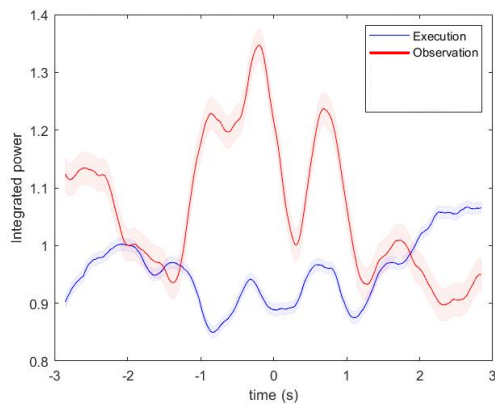
(c) Channel O1a4

Figure 9: Average power recorded by the significant electrodes in frequency band 8 Hz to 15 Hz with respect to the baseline for execution and observation tasks. The shades represent the standard deviation. Trials are aligned with ObjTouch (red vertical line on top left picture). The black vertical lines on top left picture are, from left to right: cueOn, SoundOff, ObjRelease, HandBack.

(a) Channel F12

(b) Channel F3bIb7
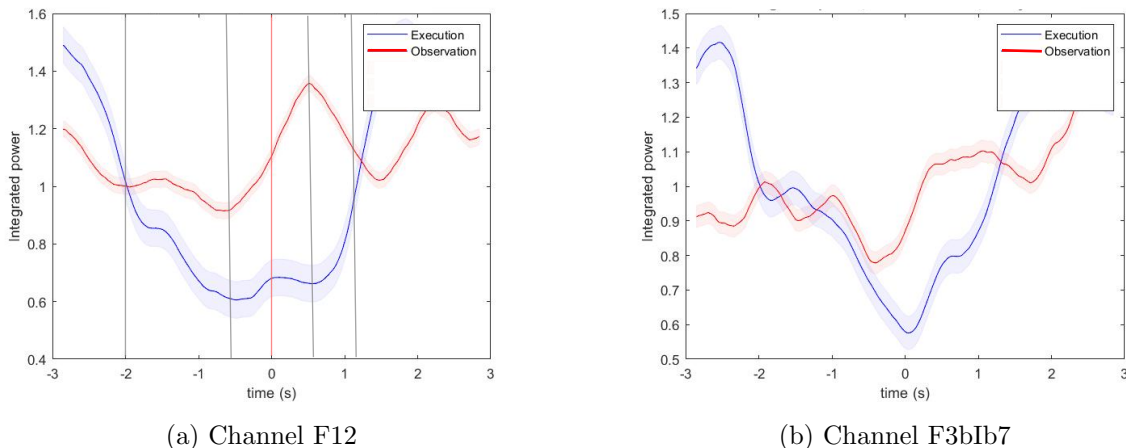
Figure 10: Average power recorded by the significant electrodes in frequency band 15 Hz to 25 Hz with respect to the baseline for execution and observation tasks. The shades represent the standard deviation. Trials are aligned with ObjTouch (red vertical line on top left picture). The black vertical lines on top left picture are, from left to right:cueOn, SoundOff, ObjRelease, HandBack.



(a) channel P1aCc9

(b) channel F2aIa16
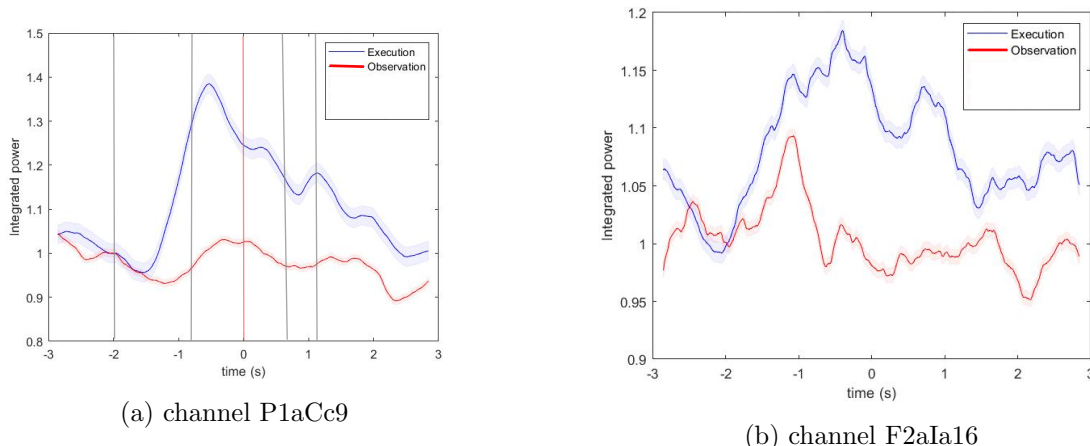
Figure 11: Average power recorded by the significant electrodes in frequency band 45 Hz to 75 Hz with respect to the baseline for execution and observation tasks. The shades represent the standard deviation. Trials are aligned with ObjTouch (red vertical line on top left picture). The black vertical lines on top left picture are, from left to right: cueOn, SoundOff, ObjRelease, HandBack

### 4.2.2 Integrated Power vs. grip type

The objective was to evaluate if and in which frequency bands the grip type is encoded. From the spectrograms, it looked like there was a difference in power modulation between object type in the high frequency range, especially for visual responses. To dig deeper into the question, the average power for each object was plotted between 45 and 70Hz both for motor and visual tasks. The results are shown in Figure 12. During observation tasks, the power increases to a different extent for the grip types: for electrode F2aIa16 (located in ctx-lh-precentral) power grip has the highest increase in power, followed by prehension grip whereas the power modulations for precision grip are much weaker (Figure 12b). This agrees with the observations we made in section **??**. On the contrary, for electrode P1aCa9,

the power rise is much more important for precision grip as compare to the two other grips (Figure 12d). The average power for each object grip was also plotted for motor tasks between 45 Hz and 70 Hz. Even though from the spectrograms, the power increased looked the same for all grip types, we can see here that precision grip also induces weaker response than prehension and power grips for electrode F2aIa1, while prehension grip induces a higher response than precision and power grips for electrode P1aCc9 (Figures 12c and 12a).

To study the effect of other frequencies on the ability to distinguish between gip types, we computed the average power in other frequency ranges. For the beta band (between 15Hz and 15Hz) for motor tasks, we find the same decrease in power during action preparation and execution for but no strong difference between grip types (Figure 15). For visual task however, we can observe two increases and two decreases in power that are slightly delayed between object types. For electrode F12, similarly to what was found for electrode F3aIa16 in the highest frequency range, the power increase is higher for power grip, followed by prehension and is weaker for precision grip and this remains consistent trhroughout the whole trial. For electrode F3bIb7 the response is higher for prehension grip until ObjRelease and becomes higher for precision grip after this event.

In the mid frequency range (8 to 15Hz), there doesn't seem to be a significant difference between grip type for motor responses (14a) but we can see a distinction for visual responses. Indeed, for visual responses, the power increase is much higher for power grip than for the two other objects (Figure 14b).

Finally, for the low frequency range (0.1 to 7Hz), for motor responses, the power modulation seems lower for power grip than for precision and prehension grip (Figure 15a) . We can also notice that the response for prehension grip is slighlty ahead compare to precision and power grips. For visual responses, the responses are much stronger for prehension and power grip as compare to precision grip (Figure 15b).

### 4.3 Statistical analysis to evaluate the difference between conditions and the ability to distinguish between grip types

The goal of this section was to answer the questions:
-"Is there a significant difference in power modulation between action execution and perception? If yes, for which specific event, frequency range and electrode?"
To examine that question, Student's unpaired t-test ($\alpha$ level of significance=0.05) were performed for each electrode in specific frequency ranges (0.1Hz to 8Hz, 8Hz to 15Hz, 15Hz to 25Hz and 45Hz to 70Hz) and time intervals (500ms around CueOn, SoundOff, ObjTouch and ObjRelease). The results of the t-test are presented in Table 5. The second question was: -"is the averaged power across trials for on grip type the same for another type in specific frequency ranges and for specific events?" To answer that question, we performed Student's unpaired t-test at a significant level of $\alpha$=0.05 between grip types for each condition and electrode in the same frequency ranges and time intervals as previously mentioned. Then, each condition, time interval and electrode was assigned a "differentiation score" that corresponds to the number of significant t-tests for that combination. The results of the differentiation score are presented in Tables 6 and 7.

We can see that there are significantly different responses between action execution and perception in $\beta$ and $\gamma$ bands during movement execution and movement preparation. We can also see that the responses are significantly different in the $\alpha$ band during action execution. However, the differences between the responses of visual and motor tasks are not significant in the low frequency range (Table 5).

As regards to distinguishing grip types, it looks like this is mainly done in the high frequency band but for motor and visual tasks. (Tables 6 and 7),
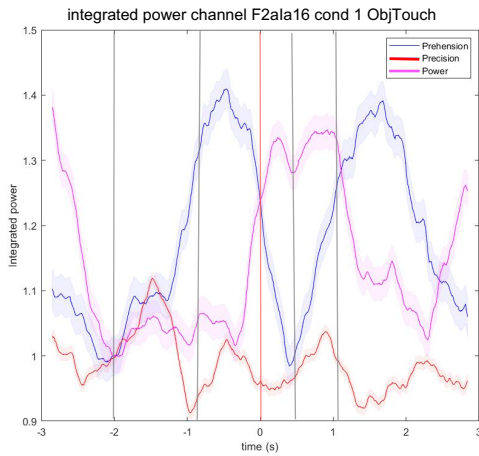
(a) Motor responses
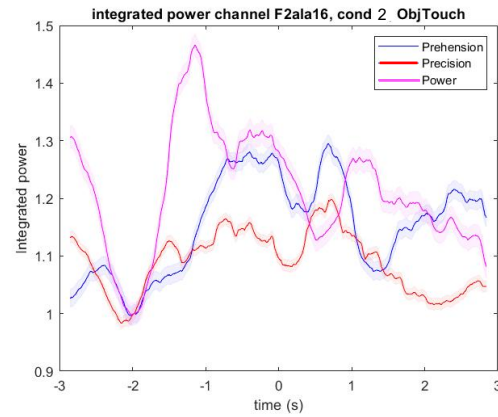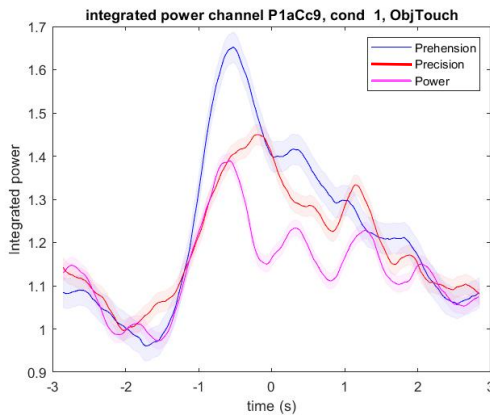
(b) Visual responses

(c) Motor responses
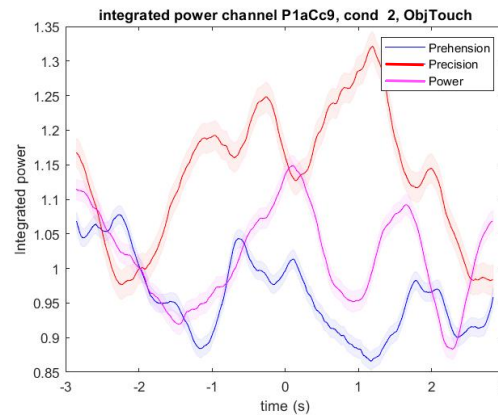
(d) Visual responses

Figure 12: Average power recorded by significant electrodes between 45 Hz and 75 Hz with respect to the baseline for execution (left) and observation (right) tasks. The shades represent the standard deviation. Trials are aligned with ObjTouch (red vertical line). The black vertical lines are, from left to right: CueOn, SoundOff, ObjRelease and HandBack
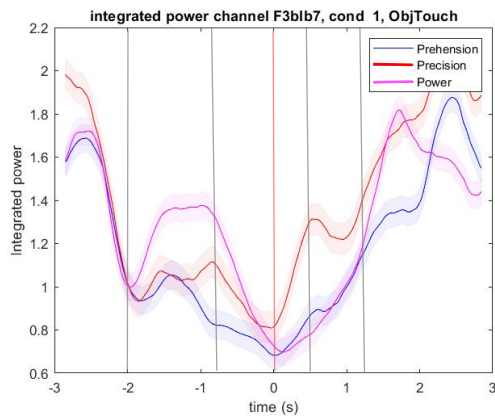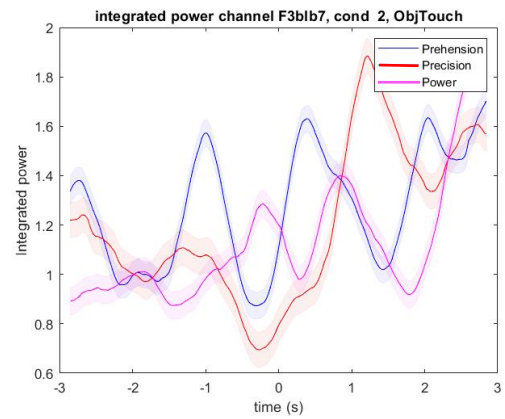
(a) Motor responses
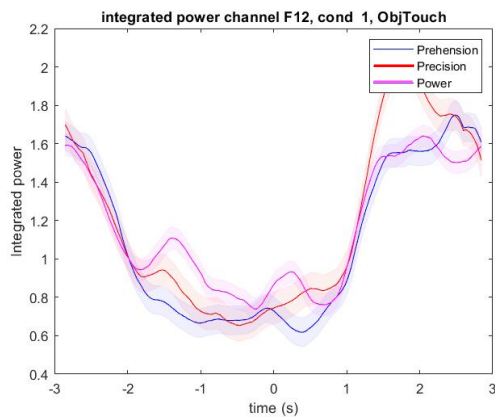
(b) Visual responses

(c) Motor responses
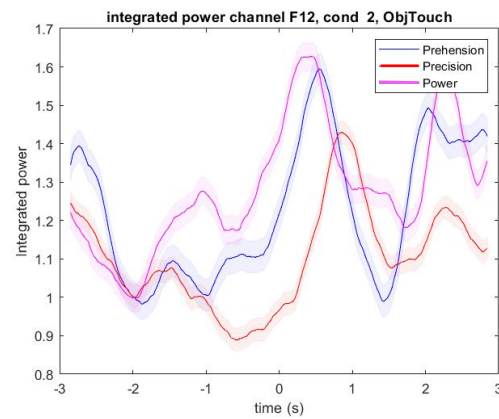
(d) Visual responses

Figure 13: Average power recorded by significant electrodes between 15 Hz and 25 Hz with respect to the baseline for execution (left) and observation (right) tasks. The shades represent the standard deviation. Trials are aligned with ObjTouch (red vertical line). The black vertical lines are, from left to right: CueOn, SoundOff, ObjRelease and HandBack

(a) Motor responses

(b) Visual responses
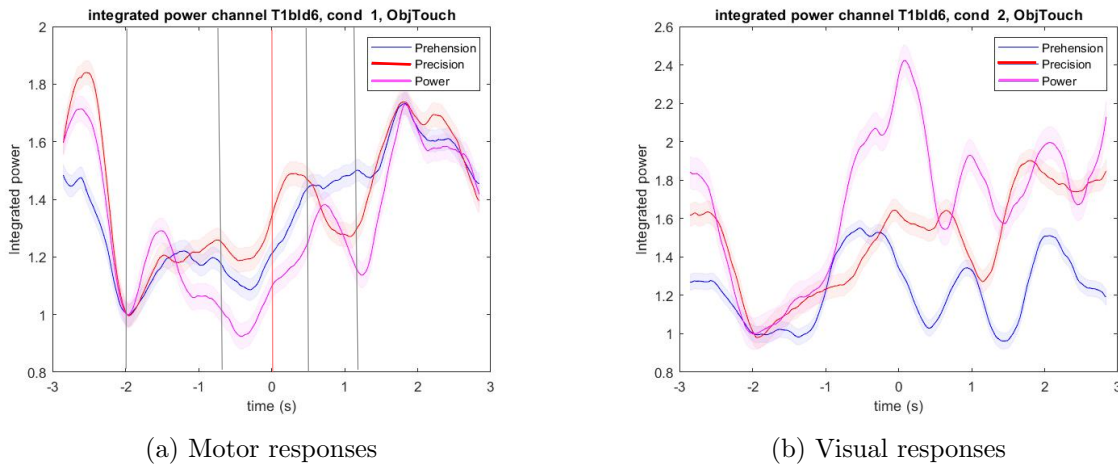
Figure 14: Average power recorded by electrode T1bId6 between 8 Hz and 15 Hz with respect to the baseline for execution (left) and observation (right) tasks. The shades represent the standard deviation. Trials are aligned with ObjTouch (red vertical line). The black vertical lines are, from left to right: CueOn, SoundOff, ObjRelease and HandBack



(a) Motor responses

(b) Visual responses
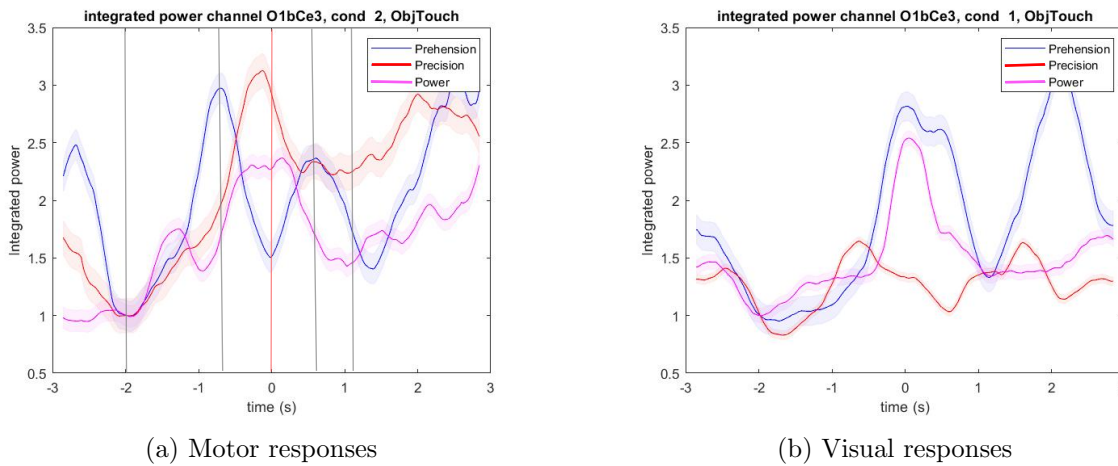
Figure 15: Average power recorded by electrode O1bCe3 between 0.1 Hz and 7 Hz for electrode T1aIc3, with respect to the baseline for execution (left) and observation (right) tasks. The shades represent the standard deviation. Trials are aligned with ObjTouch (red vertical line). The black vertical lines are, from left to right: CueOn, SoundOff, ObjRelease and HandBack

| Frequency range | Electrode | CueOn | SoundOff | ObjTouch | ObjRelease |
|---|---|---|---|---|---|
| [0.1Hz 8Hz] | T1aIc3 | 0.2771 | 0.3173 | **0.0037***  | 0.077 |
|  | O1bCe3 | 0.3677 | 0.3169 | 0.6329 | 0.7178 |
| [8Hz 15Hz] | T1bId6 | 0.4564 | 0.5734 | **0.0215** | **0.0413** |
|  | F3bId7 | 0.6745 | **0.0323** | 0.0645 | **0.0039*** |
|  | O1a4 | 0.1156 | 0.3173 | **0.0043*** | **0.0183** |
| [15Hz 25Hz] | F3bIb7 | 0.4988 | **0.0036*** | **0.004*** | **3.43e-4*** |
|  | F12 | **0.0053*** | **0.0028*** | **0.0015*** | **2.82e-5*** |
| [45Hz 70Hz] | P1aCc9 | **0.0002*** | **8.05e-7** | **4.847e-7*** | **3.73e-8*** |
|  | F2aIa16 | 0.1266 | 0.4235 | **0.0115** | 0.5093 |

Table 5: Pvalues from Student's unpaired t-test comparing motor and visual tasks. The time interval was [-0.25s 0.25s] around each event. Pvalues significant at a level $\alpha=0.05$ are in bold and pvalues significant at a level $\alpha=0.01$ are marked with a *.

| Action Execution | Electrode | CueOn | SoundOff | ObjTouch | ObjRelease |
|---|---|---|---|---|---|
| [0.1Hz 8Hz] | T1aIc3 | 0 | 0 | 0 | 0 |
|  | O1bCe3 | 0 | 0 | 0 | 0 |
| [8Hz 15Hz] | T1bId6 | 0 | 0 | 0 | 0 |
|  | F3bId7 | 0 | 1 | 0 | 0 |
|  | O1a4 | 0 | 1 | 0 | 0 |
| [15Hz 25Hz] | F3bIb7 | 0 | 0 | 0 | 0 |
|  | F12 | 0 | 0 | 0 | 0 |
| [45Hz 70Hz] | P1aCc9 | 0 | 0 | 2 | 1 |
|  | F2aIa16 | 0 | 3 | 0 | 0 |

Table 6: Differentiation score for significant electrodes in interesting frequency ranges during motor tasks. The time interval was [-0.25s 0.25s] around each event.

| Action Perception | Electrode | CueOn | SoundOff | ObjTouch | ObjRelease |
|---|---|---|---|---|---|
| [0.1Hz 8Hz] | T1aIc3 | 0 | 0 | 0 | 0 |
|  | O1bCe3 | 0 | 0 | 0 | 0 |
| [8Hz 15Hz] | T1bId6 | 0 | 1 | 0 | 0 |
|  | F3bId7 | 0 | 0 | 0 | 0 |
|  | O1a4 | 0 | 0 | 1 | 0 |
| [15Hz 25Hz] | F3bIb7 | 0 | 0 | 0 | 1 |
|  | F12 | 0 | 0 | 0 | 0 |
| [45Hz 70Hz] | P1aCc9 | 0 | 2 | 0 | 2 |
|  | F2aIa16 | 0 | 0 | 0 | 0 |

Table 7: Differentiation score for significant electrodes in interesting frequency ranges during visual tasks. The time interval was [-0.25s 0.25s] around each event.

# 5 Discussion

## 5.1 Time frequency analysis

In this project, time-frequency power spectra were analyzed between 1Hz and 100Hz to detect specific frequency ranges that could encode important information related to grasping movements and observation of the same movements. Then, we looked at the average power between conditions and grip types for specific frequency ranges.
One needs to keep in mind that we used the function "smoothdata" to do this analysis (meaning tha each sample is averaged with its neigbhors), therefore leading to a small delay in the drops or increases that can be osebrved.

From this analysis we found several noticeable frequency bands that contain different information:

**-the 45 Hz to 70 Hz frequency band contains strong power increase highly associated with motion execution and perception and is selective to grip types.**
This finding is compatible with what is described in literature. Indeed, gamma oscillations have been widely studied and have been shown to play an important role in vision and motor control, namely that power increases in gamma band is often observed during movement [24] [23]. Some studies suggest that gamma oscillations are a general cortical activity that integrates events from several areas of the cortex for a variety of cognitive processes [48] [49]. This aligns with the fact that we found an increase in power in this frequency range from electrodes in the frontal (channel F2aIa16) and parietal (channel P1aCc9) lobes.

The increase in power happens very close to motion onset (Figure 11), which corroborates the findings of several studies that propose that motor gamma oscillations could have a prokinetic role, meaning that they promote movements [26] [25] [50]. The fact that the power increase happens almost simultaneously with motion onset

suggest that gamma oscillations play a role in the driving of movements, but the evidence is unclear. However, one could wonder if the strong response that we saw around 60Hz in the spectrograms could be due to the AC line frequency, however, our signals were notch pass filtered. Plus, if that were the case, we would have seen this increase for the whole time interval and for visual responses too, whereas in our case it starts right around the event "SoundOff", stops after the event "HandBack" and is not present during action preception.

The same behavior with the same dynamic was observed during action perception, however, the responses where significantly lower than for action execution (Table 5 and Figure 11), meaning that this frequency band encodes action execution and perception similarly but is more active for motor tasks.
From the spectrograms we also noticed a difference in power increase across grip types during action perception, which led us to think that the visual responses for movement of the arm and fingers are encoded in this frequency band. This was confirmed by looking at the integrated power object by object. Indeed, we found that for both execution and observation, different grips induced different patterns in the gamma band. This is in line with the work from Prof. Kubánek et al. that showed that different movements of the hand lead to different neural activity in the high frequency band.
This could be explained by the fact that different movement types require different efforts, leading to different power outbursts. This could also be explained by looking at the placement of the electrodes. Previous studies showed that information contained in the gamma frequencies for a specific movement type are regions-specific [23] [48]. As our electrodes remains at the same location throughout the whole experiment, they would record a weaker signal if a specific movement type activates a further brain region. This can be the reason why we observeddifferent selectivity for electrode P1aCc9.
**-a power decrease between 15 Hz to 25 Hz is related to movement execution and**

**preparation whereas an increase in power is related to movement perception**

We found that action execution, preparation and action perception elicit significantly different responses in this frequency range 5.

Indeed, for action execution, we noticed an increase in power in the $\beta$ band right before movement onset, followed by a drop in power during action execution, and a increase again after movement until recovery of the power to baseline level (Figure 10). This corresponds to what is describe in literature as the "$\beta$-rebound" [35] [36] [51]. This terms refers to the observation that preparation and execution of voluntary movements result in a block of oscillations in the motor area in frequency bands around 15 Hz to 25 Hz. A decrease in power compare to baseline can be refered to as an event-related desynchronization [52] [53]. This negative power modulation in the beta band is opposite to the power peak observe in the gamma band which corroborates the findings of several studies which suggest that beta activity presents an inhibitory role that regulates gamma activity [28].

For action perception on the other hand, we can see the same behavior (drop in power followed by a power increase), but much weaker and with a different dynamic. Therefore This frequency range does not encode for specific grip type as there are no statistical significance when comparing objects in this band (Figures 6 and 7).

**Modulations of the neuronal responses between 0.1 Hz-8 Hz and 8 Hz-15 Hz seems to be related to movement and are similar between action perception and action execution** We observed two power increases during motion execution and perception, corresponding to when the participant (being the patient for execution task and the experimenter during observation task) leaves the hand resting plate to grab the object (interval between SoundOff and ObjTouch) and when the patient removes his hand from the object to reach the hand resting plate again. These modulations of neuronal responses were similar and happening with the same dynamic during action execution

and action perception (Figures 8 and 9) and there wasn't any significant difference between the two conditions 5. The stronger response observed for visual task compared to motor task in some channels can be explained by looking at the location of the electrodes. Indeed, channel O1bCe3 and O1a4 are both localized in the occipital lobe which contains most of the regions of the visual cortex and is primarily responsible for visual processing [54]. Channels T1bId6 and T1aIc3 are both in the superior temporal gyrus, which is typically associated with the auditory cortex and to processing sounds, but studies also suggested that it playes a role in visual processing. Indeed, the superior temporal cortex seems to be the region in which lesions cause spatial neglect [55].

This frequency range does not entail information allowing to distinguish between grip types (Figures 6 and 7) .

## 5.2 General discussion about the experiment

The main problem that we encountered with our experience was that all trials were not perfectly aligned in terms of events. Indeed, the patient performed the task at his own pace, which differs from trial to trial giving rise to a big temporal variability from trial to trial. Indeed, in contrast with vision experience where the timing is very specific and always the same for all trials, in our case, the patient's reaction vary over time. Therefore, when averaging across trials, due to this misalignment, trials may cancel each other out. That is why it was necessary to also study spectrograms on a trials by trials basis, to see if there is was consistent pattern between trials that may not appeared on the spectrogram averaged across trials. In annex is presented the spectrograms trials by trials for electrodes FaCa2, FaCa6 and FaCa8 (Figures 19, 20, 21, 22, 23 and 24) for motor and visual responses. We can see that the spectrograms on a trial by trial basis look very different than the averaged spectrograms, however, no consistent pattern could be detected.

During the first trials the patient was learning the task, which might disrupt the rest of the trials. This is very visible in Figure 16 where we can see that the first 5 trials are very noisy as compared to the rest, probably corresponding to the learning phase where the patient learns and integrate the task. For later experiment. When collecting data from other patients, one should do some practice trials before starting the experiment to remove this effect.

Furthermore, it should be emphasized that our mapping of brain locations is quite extensive but not exhaustive and that we do not chose the location of electrodes' used. The location of electrodes is determined by the surgeons to meet their clinical requirements. Moreover, this study uses IFPs which combine the activities coming from of several neurons.

Finally, when looking at these results, we should take into consideration that the data was recorded from a single patient, which can questioned the significance of this study. To confirm or refute these findings, and make sure of the fact that our results are not due to external factors, more data from more patients need to be collected.

lates gamma activity .

This neural modulations are visible not only during motor responses but also during the visual responses, for different regions of the brain, implying that action execution and action perception activate the same processes in humans.

Gamma bands oscillations allow to significantly distinguish between grip types, meaning that this frequency range encode for the intermediate goal of an observed action, which was found to be particularly the case in parietal area.

Even though this study was only conducted on one patient, it gives promising results and more data should be collected in order to confirm or refute these findings.

This project gave a first insight in understanding the neural mechanisms underlying action perception and execution.

Knowledge of these mechanisms can have high significance in several fields : clinical practive, brain=machine interface, Human-robot interactions. The implications are numerous. Over the past decade, more research has suggested that mirror neurons might help explain not only empathy, but also autism and even the evolution of language [9] [56] [6].

## 6. Conclusion

In this project, neural mechanisms underlying action execution and action perception were studied and compared thanks to recordings from SEEG electrodes implanted in humans.

Four frequency bands of special interest were identified: High frequencies (between 45 and 70 Hz-gamma band) present positive power burst related to movement (when reaching and grabbing an object and when coming back to initial position). Low to mid frequencies also induce a power peack related to movement. A power decrease in the 15 Hz to 25 Hz range is linked to movement preparation and execution and regu-

# 7   Annexes



Figure 16: IFP across all trials from the sixth deepest channel on electrode F3aCa located in the left cerebral white matter. These are the results aligned with event ObjTouch and for the first object (prehension grip)

| Parameter | Event it corresponds to |
|---|---|
| BlockStart | Moment when the block starts. |
| TrialStart | Moment at which the trial begins. |
| HandRestTime | Interval of time between trialStart and CueOn during which the participant must keep their hand on the hand resting plate. |
| CueOn | Moment where one of the LEDs turns on, indicating which object to grab. |
| CueOff | Moment where the LED turns off. |
| CueDuration | Interval of time between CueOn and CueOff (500ms) |
| SoundOn | Moment where the sounds starts to play (same time as CueOn) |
| SoundOff | Moment where the sounds stops playing, indicating the participant that they can go and grab the object |
| SoundDuration | Interval of time between SoundOn and SoundOff (1.5 2.5s) |
| HandOut | Moment where the participant no longer touches the hand resting plate. |
| ObjTouch | Moment at which the participant touches the object. |
| ObjRelease | Moment at which the participant no longer touches the object. |
| HandBack | Moment where the participant places their hand back on the hand resting plate. |
| TrialEnd | Moment at which the trials ends. |
| DiscardKey | This value is **0** by default and becomes **1** if an external factor disrupted the trial. |
| ErrorCode | This value indicates if an error occured during the trial and which one.It takes the values: **0** by default: no error. **-1**: the participant grabbed the wrong object. **1**: too slow, maximal duration exceeded. **2**: premature arm movement during cue presentation. **4**: not keeping their hand on the hand resting plate during the HandRestTime. |
| ObjCode | This value indicates which object was supposed to be grabbed. it takes the values: **1** for prehension grip, **2** for precision grip and **3** for power grip. |
| Triggers | Several Triggers were sent: **Tigger Block**:1 at the beginning of each block indicating if it's an observation or execution task 3 triggers to differentiate between block. **Trigger Start** at the begining of each trial **Trigger** LED is sent during CueOn **Trigger Touch** is sent when the participant grabbed an object. **Trigger Handback** is sent when the participant places their hand on the hand resting plate. **Trigger WrongObject** is sent if the object touched by the participant differs from the one indicated by the LED. For each of these triggers we record their number and duration. |

Table 8: Description of the parameters used and saved for each trial during the experiment. 'Participant' designates the patient for motor task and the experimenter during observation task.

| Electrode Name | Electrode | Anchor (mm) | Initial Robot-Target, A | Final Robot-Target | Scalp - Dura Distance | Trajectory Length (mm) | Drill Length, B | Distance to Screw, C | Electrode Length, D |
|---|---|---|---|---|---|---|---|---|---|
| O1a | 2102-06-091 | 25 | 110 | 180 | 15 | 20.9 | 159 | | 180 |
| P2b | 2102-06-091 | 35 | 111 | 180 | 17 | 19.6 | 160 | | 180 |
| T2 | 2102-06-091 | 25 | 108 | 180 | 13 | 20.6 | 159 | | 180 |
| T3H | 2102-12-091 | 25 | 129 | 180 | 12 | 43.1 | 137 | | 180 |
| T1aIc | 2102-08-091 | 25 | 117 | 180 | 14 | 29 | 151 | | 180 |
| F3aCa | 2102-16-091 | 25 | 146 | 180 | 14 | 57.9 | 122 | | 180 |
| F3bIb | 2102-08-091 | 25 | 115 | 180 | 12 | 29 | 151 | | 180 |
| T1bId | 2102-10-091 | 25 | 122 | 180 | 13 | 34.7 | 145 | | 180 |
| F2bCb | 2102-14-091 | 25 | 137 | 180 | 12 | 50.9 | 129 | | 180 |
| P2a | 2102-08-091 | 25 | 116 | 180 | 14 | 27.6 | 152 | | 180 |
| O1bCe | 2102-14-091 | 35 | 140 | 180 | 17 | 48.9 | 131 | | 180 |
| P1bCd | 2102-12-091 | 35 | 134 | 180 | 16 | 43.7 | 136 | | 180 |
| P1aCc | 2102-14-091 | 25 | 137 | 180 | 14 | 49.1 | · 131 | | 180 |
| F1 | 2102-10-091 | 25 | 123 | 180 | 14 | 34.7 | 145 | | 180 |
| F2aIa | 2102-16-093 | 25 | 158 | 180 | 13 | 71.3 | 109 | | 180 |

Figure 17: Characteristics of electrodes implanted
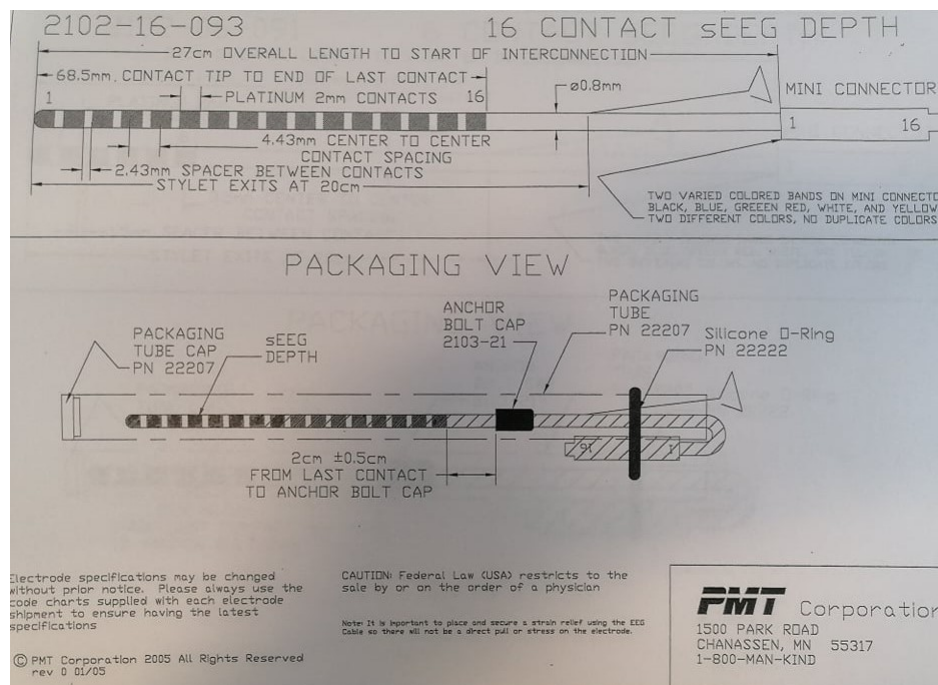


Figure 18: Diagram of SEEG electrode used for experiment
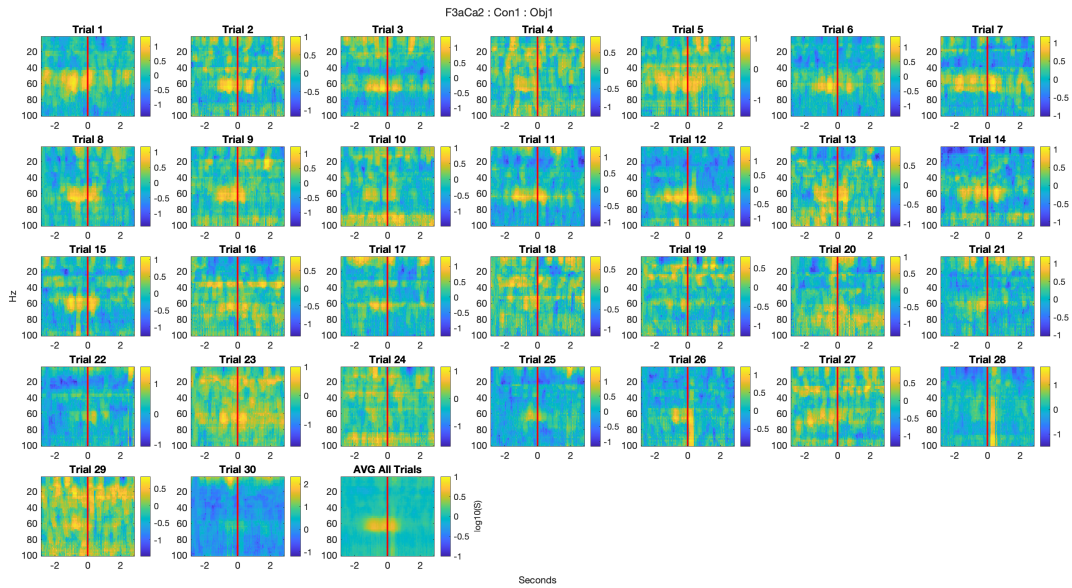
Figure 19: Time-frequency analysis of the motor responses from electrode F3aCa2, located in ctx-lh-posteriorcingulate, for all trials, for object 1 (prehension grip). The tasks were aligned with ObjTouch
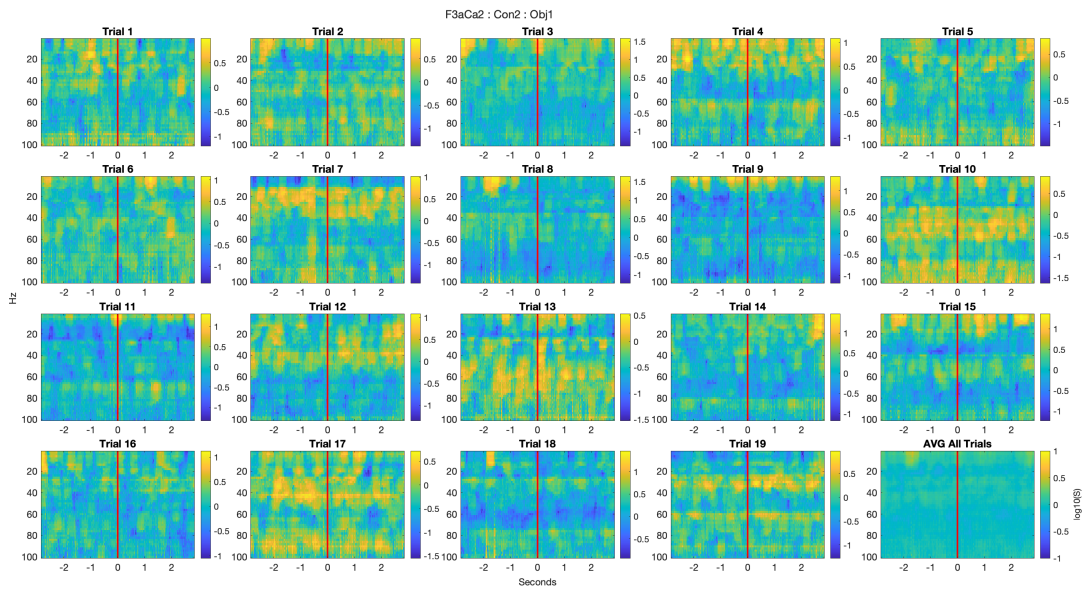


Figure 20: Time-frequency analysis of the visual responses from electrode F3aCa2, located in ctx-lh-posteriorcingulate, for all trials, for object 1 (prehension grip). The tasks were aligned with ObjTouch
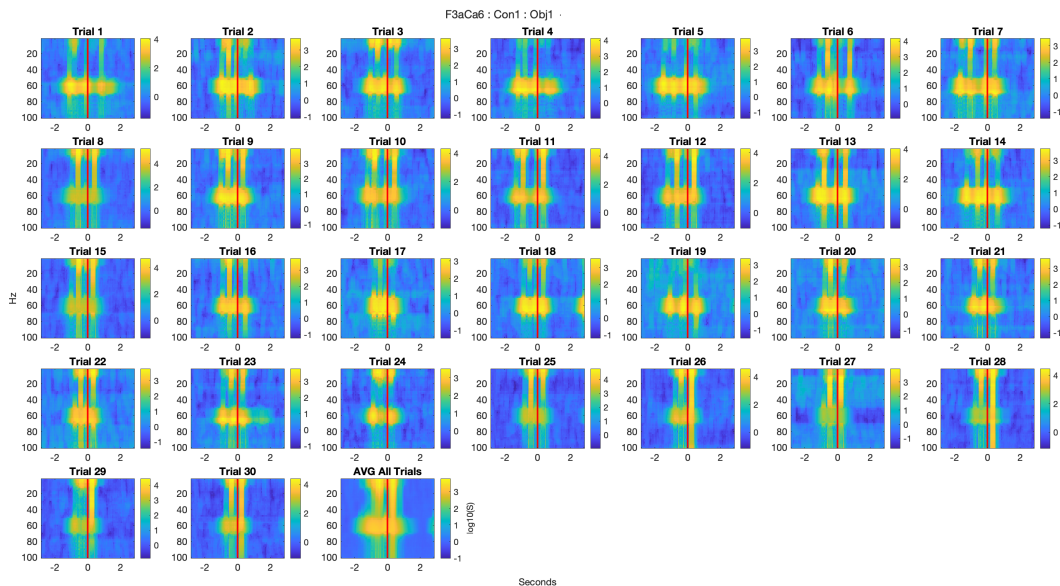
Figure 21: Time-frequency analysis of the motor responses from electrode F3aCa6, located in the Left-Cerebral-White-Matter, for all trials, for object 1 (prehension grip). The tasks were aligned with ObjTouch
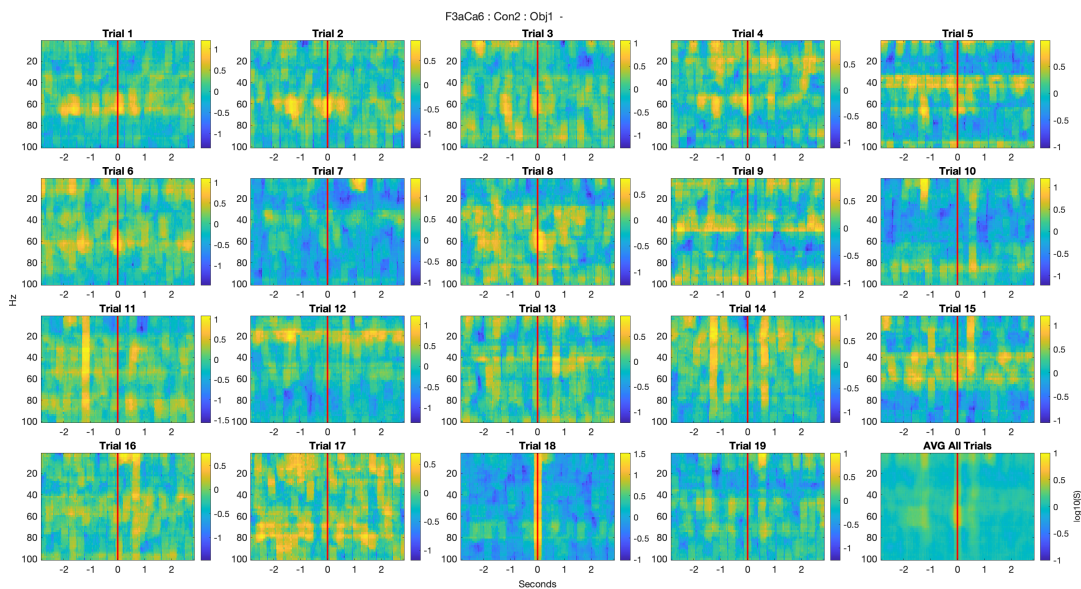


Figure 22: Time-frequency analysis of the visual responses from electrode F3aCa6, located in the Left-Cerebral-White-Matter, for all trials, for object 1 (prehension grip). The tasks were aligned with ObjTouch
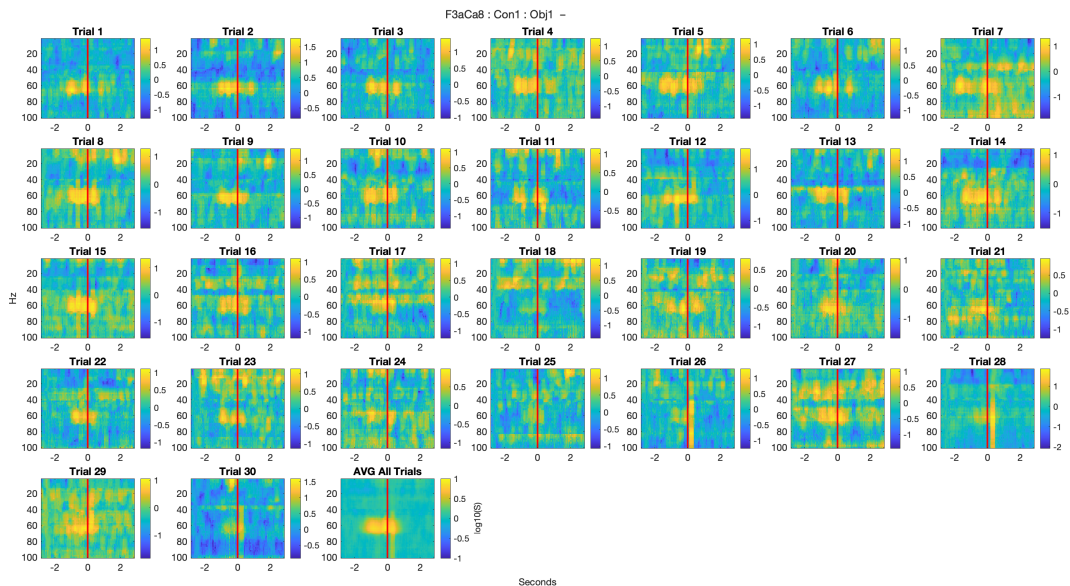
Figure 23: Time-frequency analysis of the motor responses from electrode F3aCa8, located in the Left-Cerebral-White-Matter, for all trials, for object 1 (prehension grip). The tasks were aligned with ObjTouch
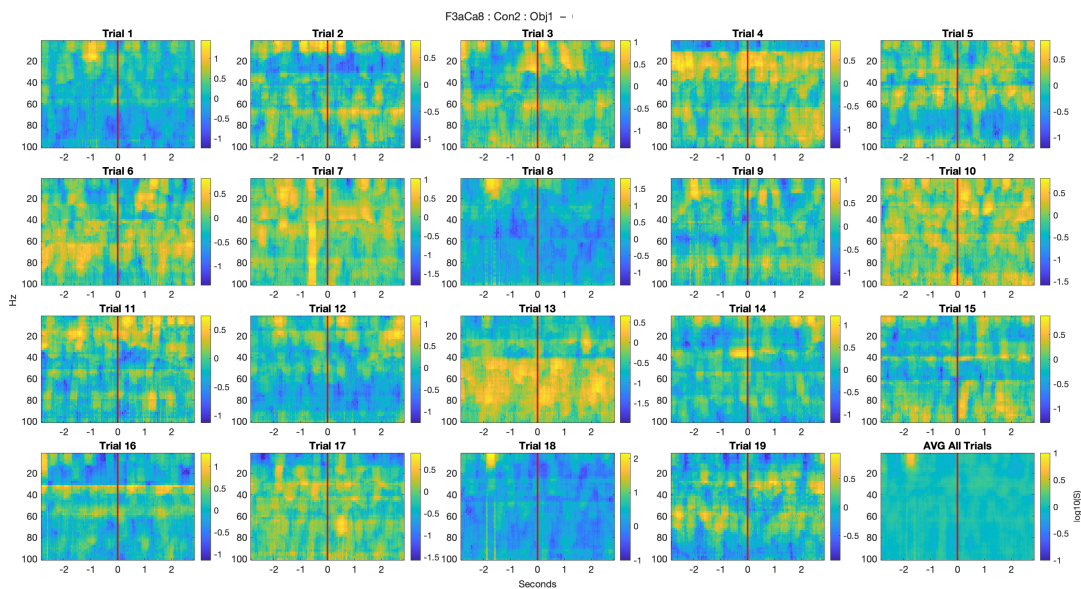


Figure 24: Time-frequency analysis of the visual responses from electrode F3aCa8, located in the Left-Cerebral-White-Matter, for all trials, for object 1 (prehension grip). The tasks were aligned with ObjTouch

# References

[1] Harold Bekkering Natalie Sebanz and Gunther Knoblich. Joint action: bodies and minds moving together. *Trends in Cognitive Sciences*, 10(2), 2006.

[2] G. Rizzolatti and L.Craighero. The mirror neuron system. *Annual Rev Neurosci*, 27(169-192), 2004.

[3] Cecilia Heyes. Mesmerising mirror neurons. *Neuroimage*, 2016.

[4] L Fogassi V Gallese G Rizzolatti G di Pellegrino, L Fadiga. Understanding motor events: a neurophysiological study. *Experimental Brain Research*, 91(1):176–180, 1992.

[5] Fabian Chersi. Neural irroechanisms and models underlying joint action. *Experimental Brain Research*, 211, 2011.

[6] Lea Winerman. The mind's mirror, 2005.

[7] Fogassi L. Gallese V., Fadiga L. and Rizzolatti G. Action representation and the inferior parietal lobule. *In Prinz W. and Hommel B., Common Mechanisms in Perception and Action: Attention and Performance, Oxford: Oxford University Press*, 19:334–355, 2002.

[8] Gesierich B. Chersi F. Fogassi L., Ferrari P. and Rizzolatti G. Parietal lobe: From action organization to intention understanding. *Science*, 308:662–667, 2005.

[9] K. Nakahara and Y. Miyashita. Understanding intentions: Through the looking glass. *Science*, 308:644–645, 2005.

[10] Gentilucci M. and Rizzolatti G. Cortical motor control of arm and hand movements. *Vision and action: the control of grasping*, pages 147–162, 1990.

[11] Leonardo Fogassi Giacomo Rizzolatti Vittorio Gallese, Luciano Fadiga. Action recognition in the premotor cortex. *Brain*, 119:553–609, 1996.

[12] Rizzolatti G Gallese V, Keysers C. A unifying view of the basis of social cognition. *Trends in Cognitive Sciences*, 8:396–403, 2004.

[13] G. Pavesi L. Fadiga, L. Fogassi and G. Rizzolatti. Motor facilitation during action observation: a magnetic stimulation study. *Journal of Neurophysiology*, 73(6):2608–2611, 1995.

[14] C.D. Frith and U. Frith. Interacting minds-a biological basis. *Science*, 1999.

[15] J. Rowe J. Grezes, J.L. Armony and R.E. Passingham. Activations related to "mirror" and "canonical" neurones in the human brain: an fmri study. *NeuroImage*, 18:929–937, 2003.

[16] Marcel Brass Harold Bekkering John C. Mazziotta Giacomo Rizzolatti Marco Iacoboni, Roger P. Woods. Cortical mechanisms of human imitation. *Science*, 286(5449):2526–2528, 1999.

[17] H. Huang E. Montgomery S.V. Sarma D. Huberdeau, H. Walker. Analysis of local field potential signals: a systems approach. *Annual International Conference of the IEEE Engineering in Medicine and Biology Scociety*, 2011.

[18] S. Panzeri A. Mazzoni, N.K. Logothetis. The information content of local field potentials: experiments and models. 2012.

[19] S. Man D. Hong S.X. Moffett, S.M. O'Malley and J.V. Martin. Dynamics of high frequency brain activity. *Scientific Reports*, 7, 2017.

[20] A. Kawiak L. Kwasniewicz P. Schneider N. Polak G.M. Wojcik, J. Masiak and A. Gajos-Balinska. Mapping the human brain in frequency band analysis of brain cortex electroencephalographic activity for selected psychiatric disorders. *Frontiers in NeuroInformatics*, 2018.

[21] W.Gawali Suresh C.Mehrotra Priyanka A.Abhang, Bharti. Introduction to eeg- and speech-based emotion recognition. *SciendeDirect*, page 51–79, 2016.

[22] C. Magri Y. Murayama M.A. Montemurro N.K. Logothetis A. Belitski, A. Gretton and S. Panzeri. Low-frequency local field potentials and spikes in primary visual cortex convey independent visual information. *Journal of Neuroscienc*, 28:5696–5709, 2008.

[23] I. Mutschler E. Neitzel C. Mehring K. Vogt A. Aertsen A. Schulze-Bonhage T. Ball, E. Demandt. Movement related activity in the high gamma range of the human eeg. *NeuroImage*, 41, 2008.

[24] José Luis Ulloa. The control of movements via motor gamma oscillations. *Frontiers in Human Neurosciences*, 2022.

[25] Bells S. Ferrari P. Gaetz W. Cheyne, D. and A. C. Bostan. Self-paced movements induce high-frequency gamma oscillations in primary motor cortex. *NeuroImage*, 42:332–342, 2008.

[26] Miglioretti D. L. Gordon B. Sieracki J. M. Wilson M. T. Uematsu S.-et al. Crone, N. E. Functional mapping of human sensorimotor cortex with electrocorticographic spectral analysis. i. alpha and beta event-related desynchronization. *Brain A J. Neurol.*, 121:2271–2299, 1998.

[27] Leuthardt E. C. Schalk G. Rao R. P. N. Anderson N. R. Moran-D. W. et al. Miller, K. J. Spectral changes in cortical surface potentials during motor movement. *J. Neurosci.*, 27:2424–2432, 2007.

[28] G. Pfurtscheller and C. Neuper. Simultaneous eeg 10 hz desynchronization and 40 hz synchronization during finger movements. *NeuroReport*, 3:1057–1060, 1992.

[29] Schölkopf B. Grosse-Wentrup, M. and J. Hill. Causal influence of gamma oscillations on the sensorimotor rhythm. *NeuroImage*, 56:837–842, 2011.

[30] Schalk G. Fetz E. E. den Nijs M. Ojemann J. G. Miller, K. J. and R. P. N. Rao. Cortical activity during motor execution, motor imagery, and imagery-based online feedback. *Proc. Natl. Acad. Sci. U.S.A.*, 107:4430–4435, 2010.

[31] Graimann B. Huggins J. E. Levine S. P. Pfurtscheller, G. and L. A. Schuh. Spatiotemporal patterns of beta desynchronization and gamma synchronization in corticographic data during self-paced movement. *Clin. Neurophysiol*, 114:1226–1236, 2003.

[32] G. Pfurtscheller. Central beta rhythm during sensorimotor activities in man. *Electroencephalogr. Clin. Neurophysiol.*, 51:253–264, 1981.

[33] R. Salmelin and R. Hari. Spatiotemporal characteristics of sensorimotor neuromagnetic rhythms related to thumb movement. *Neuroscience*, 60:537–550, 1994.

[34] W. Prinz. Perception and action planning. *Eur. J. Cogn. Psychol.*, 9:129–154, 1997.

[35] Gaetz W. C. Bostan A. C. Jurkiewicz, M. T. and D. Cheyne. Post-movement beta rebound is generated in motor cortex: evidence from neuromagnetic recordings. *NeuroImage*, 32:1281–1289, 2006.

[36] A. K. Engel and P. Fries. Beta-band oscillations—signalling the status quo? *Curr. Opin. Neurobiol.*, 20:156–165, 2010.

[37] R.T. Knight R.T. Canolty. The functional role of cross-frequency coupling. *Trends in Cognitive Sciences*, 14:506–515, 2010.

[38] Lara Jehi. The epileptogenic zone: Concept and definition. *Epilepsy Currents*, 18:12–16, 2018.

[39] Sreejith Hrishikesan. Advantages, disadvantages and applications of eeg, 2018.

[40] P. Shah A. Revell I.Z. Ong L.G. Kini J.M. Stein R.T. Shinohara-T.H. Lucas K.A. Davis J.M. Bernabei, T.C. Arnold. Electrocorticography and stereo eeg provide distinct measures of brain connectivity: implications for network models. *Brain Communications*, 3, 2021.

[41] S.E. Paraskevopoulou M. Wang Y. Xu Z. Wu L. Chen D. Zhang G. Li, S. Jiang and G. Schalkc. Optimal referencing for stereo-electroencephalographic (seeg) recordings. *Neuroimage*, 183:327–335, 2018.

[42] F. Cardinale et al. Implantation of stereoelectroencephalography electrodes: A systematic review. *Journal of Clinical Neurophysiology*, 33:490–502, 2016.

[43] Neurological Surgery University of Pittsburgh, School of Medicine. Stereoelectroencephalography (seeg).

[44] and P. Kubben C. Herff, D.J. Krusienski. The potential of stereotactic-eeg for brain-computer interfaces: Current progress and future directions. *Frontiers in Neuroscience*, 14, 2020.

[45] D. H. Brainard. The psychophysics toolbox. *Spatial Vision*, 10:433–436, 1997.

[46] J.E. Kulkarni S. Mehta H. Bokil, P. Andrews and P. Mitrab. Chronux: A platform for analyzing neural signals. *Journal of Neuroscience Methods*, 192:146–151, 2010.

[47] E.F. Chang J.J. Lin J. Parvizi A. Perry, J. Stiso and R.T. Knight. Mirroring in the human brain: Deciphering the spatial-temporal patterns of the human mirror neuron system. *Cerebral Cortex*, 2017.

[48] S. L. Bressler. The gamma wave: a cortical information carrier? *Trends Neurosci.*, 13:161–162, 1990.

[49] P. Fries. A mechanism for cognitive dynamics: neuronal communication through neuronal coherence. *Trends Cogn. Sci.*, 9:474–480, 2005.

[50] Scherer R. Ojemann J. G. Rao R. P. Miller K. J. Darvas, F. and L. B. Sorensen. High gamma mapping using eeg. *NeuroImage*, 49:930–938, 2010.

[51] Trachel R. Kilavik B. E. Zaepffel, M. and T. Brochier. Modulations of eeg beta power during planning and execution of grasping movements. *PLoS One*, 2013.

[52] G. Pfurtscheller and F. H. Lopes daSilva. Event-related eeg/meg synchronization and desynchronization: basic principles. *Clinical Neurophysiology*, 110:1842–1857, 1999.

[53] ∗ Ross E. Vanderwert b Valentina Sclafani c Annika Paukner d Elizabeth A. Simpson e Stephen J. Suomi d Nathan A. Fox f Fabrizia Festante, a and g Pier Francesco Ferraria. Eeg beta desynchronization during hand goal-directed action observation in newborn monkeys and its relation to the emergence of hand motor skills. *Dev Cogn Neurosci*, 30:142–149, 2018.

[54] Yasir Al Khalili Amna Rehman. Neuroanatomy, occipital lobe. *StatPearls[Internet]*, 2021.

[55] Hans-Otto Karnath. New insights into the functions of the superior temporal cortex. *Nature Reviews Neuroscience*, 2:568–576, 2001.

[56] Mirror, mirror in the brain: Mirror neurons, self-understanding and autism research, 2007.